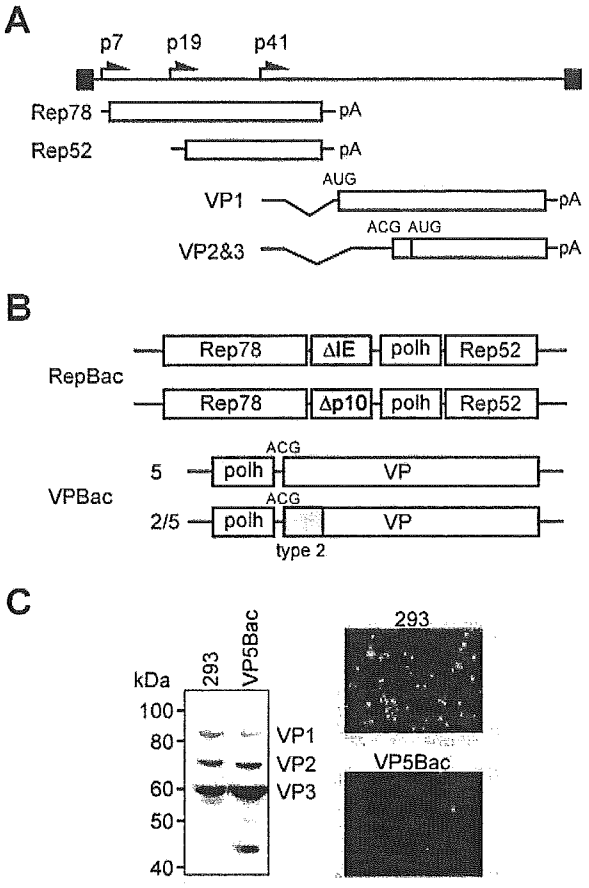

FIG. 2. (A) Genetic and transcriptional map of type 5 AAV. The p7 and p19 promoters drive Rep78 and Rep52, respectively. The p41 promoter transcribes two mRNAs. One expresses VP1, and the other is for VP2 and VP3. The initiation codon for VP2 is ACG, which is poorly utilized for translation, leading to production of a smaller amount of VP2 polypeptides than VP3 polypeptides. The ITRs are indicated by black boxes. pA, polyadenylation signal sequence. (B) Recombinant baculoviruses (rBac) constructed. An rBac for Rep utilizes a truncated promoter for the immediate-early 1 gene of *Orgyia pseudotsugata* nuclear polyhedrosis virus (ΔIE) for type 5 Rep78, and another RepBac expresses Rep78 under the control of a truncated p10 promoter (Δp10). See Fig. 4A for details. Either RepBac uses the polyhedrin promoter (polh) for Rep52. For expression of type 5 capsid proteins, a recombinant baculovirus that harbored a VP gene on which the initiation codon for VP1 is mutated to ACG was constructed (VP5Bac). Another series of VPBacs that had the type 5 VP1 gene partially replaced by the corresponding portion of type 2 VP1 at the N terminus was generated. (C) Western analysis of Sf9 cells infected with VP5Bac. The initiation codon for VP1 was mutated to an ACG codon, which enabled synthesis of VP1, -2, and -3 from a single VP mRNA. The amount of VP1 synthesized was extremely small compared to that in 293 cells. rAAV5-GFP generated with VP5Bac was used for the infection of COS cells at 10^5 vg per cell. The number of GFP-positive cells was 10% of the number of positive cells obtained with rAAV5-GFP produced in 293 cells.

peptides produced with VP251Bac through VP256Bac. Each VPBac produced chimeric VP1 at levels comparable to those of VP2. Formation of empty capsids was confirmed by CsCl density gradient analysis of Sf9 cell lysate infected with VP254Bac, as shown in Fig. 3C. The peak of VP polypeptides came to the fraction of 1.31 g/cm^3, a buoyant density of empty capsids. The GFP gene between the type 5 ITRs could be packaged into each type of chimeric capsid, and all of the chimeric rAAV5-GFPs except VP251 could transduce COS cells with efficiency similar to that of 293 cell-produced rAAV5-GFP (data not shown). The yields of rAAV5-GFP produced with VP253Bac or VP254Bac were approximately 1.2 times higher than others, although the difference was not statistically significant. We thus used VP254Bac to produce rAAV5 for the next experiments.

The initial Rep baculovirus for type 2 rAAV production drove type 2 Rep72 expression with a truncated promoter for the immediate-early 1 gene of *Orgyia pseudotsugata* nuclear polyhedrosis virus (ΔIE) and type 2 Rep52 under the control of the polyhedrin promoter (31) (Fig. 2B). The AAV5 genome encodes nonstructural proteins Rep78 and Rep52 (Fig. 2A). Similarly, we constructed a Rep baculovirus that expressed type 5 Rep78 and Rep52 under the control of the ΔIE promoter and the polyhedrin promoter, respectively. The titers of the type 2 or type 5 Rep baculoviruses, however, were lower than those of other recombinant baculovirus vectors (e.g., VPBac, GFPBac). The immediate-early 1 gene promoter becomes active at the early stage of baculovirus infection, and we thought that early expression of Rep78 in insect cells might negatively affect the yields of recombinant baculoviruses. The very late p10 promoter, which is widely used for recombinant protein production, is active at the latest stage of baculovirus infection. Thus, to delay and suppress the expression of Rep78, we tested a series of truncated p10 promoters. First, we screened the truncated p10 promoters for production of type 2 rAAV and selected one that generated high-titer rAAV2. Figure 4A shows the map of the p10 promoter and the truncated p10 promoter we constructed. The upstream TAAG sequence does not affect the activity of the p10 promoter (32). The sequence between the TAAG sequence and the p10 protein initiation codon at +72 (where the transcription start site is defined as +1) is called the burst sequence and is required for the "burst" of expression of the p10 protein at the very late stage of baculovirus infection. The *vlf-1* transactivator interacts with the burst sequence and strongly stimulates the transcription from the p10 promoter (35). To construct a weak p10 promoter (Δp10), we removed the burst sequence between positions +39 and +72 from the original p10 promoter. The Δp10 promoter was best for the production of rAAV2 among a series of truncated p10 promoters we examined. The titers of recombinant baculoviruses with the Δp10 promoter were comparable to those of other recombinant baculoviruses. The Δp10 promoter was transferred to express type 5 Rep78 (Fig. 2B). Figure 4B compares the time courses of type 5 Rep expression by ΔIE and Δp10 promoters over 72 h after infection, indicating that the Δp10 promoter-driven Rep78 expression was detected at 24 h after infection while the ΔIE promoter expressed Rep78 as early as 12 h after infection. To examine whether this modest difference in the levels of Rep78 affected replication of the AAV vector DNA, we isolated the low-molecular-weight DNA from the Sf9 cells infected with hGFP baculovirus and a Rep baculovirus (Fig. 4C). A ladder of replicative forms (RF) of rAAV5 DNA began to appear at 36 h postinfection in either case. The expected size of rAAV5-hGFP or monomer RF is 2.4 kb and the sizes of dimer and trimer RF are 4.8 and 7.2 kb, which is consistent with the result of the agarose gel electrophoresis.

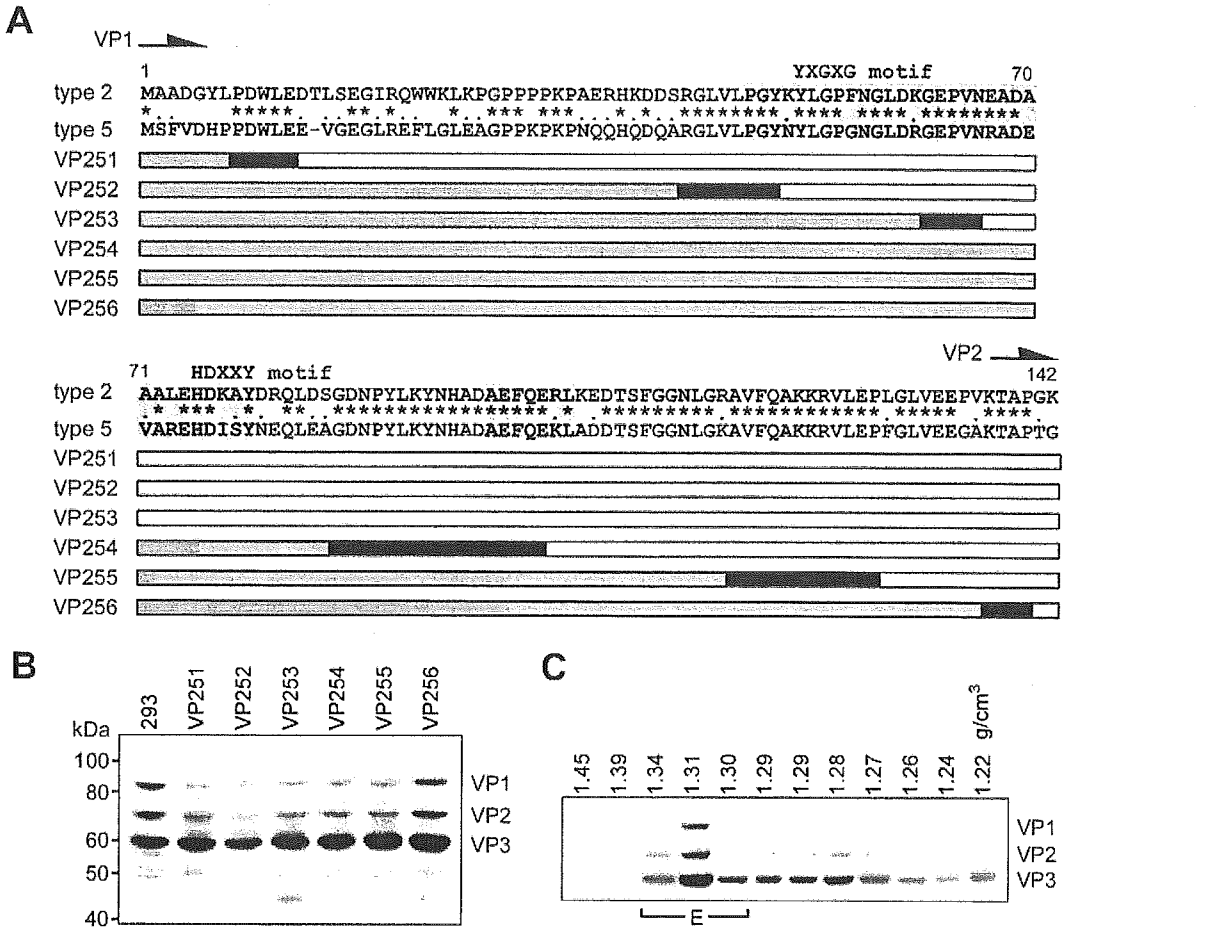

FIG. 3. (A) Chimeric VP genes constructed. The portions derived from type 2 are indicated in gray, while those from type 5 are in white. The common portions are indicated in black. The phospholipase A_2 motifs are shaded. The YXGGX and HDXXY motifs (where X is any amino acid residue), indicating the catalytic site and Ca^{2+} binding loop, respectively, are also shown. The amino acid residues common between type 2 and type 5 are indicated by asterisks. Amino acid residues classified into the same group are indicated by dots. (B) Expression of chimeric VP polypeptides in Sf9 cells. One microgram of cell lysate was resolved onto a 4 to 12% NuPAGE Bis-Tris gel in MOPS (morpholinepropanesulfonic acid) buffer (Invitrogen). Separated proteins were transferred to a Durapore membrane (Millipore), and VP proteins were detected with a rabbit polyclonal antibody raised against the type 5 VP3 portion. The lane labeled 293 shows lysate from HEK 293 cells transfected with pSR487, a hybrid plasmid harboring type 5 AAV *rep* and *cap* genes and adenovirus E2A, VA RNA, and E4orf6 genes (27). Lanes labeled VP251 through VP256 indicate lysates from Sf9 cells infected with recombinant baculovirus expressing chimeric VP. (C) Chimeric VP between types 2 and 5 is able to form empty particles. Sf9 cells (1×10^7 cells) infected with a VP2/5Bac, VP253Bac, were lysed as described in Materials and Methods. Solid CsCl was added to make a buoyant density of 1.30 g/cm^3. After ultracentrifugation for 24 h at 36,000 rpm at 21°C using an SW40 Ti rotor (Beckman), 1-ml fractionations were collected. A portion of each fraction was resolved onto a 4 to 12% NuPAGE gel in MOPS buffer, transferred to a Durapore membrane, and detected with a rabbit anti-type 5 VP polyclonal antibody. The buoyant density of each fraction is indicated above each lane. Fractions that contain empty capsids are indicated by E.

Heteroserotypic small Rep can package rAAV5 DNA into type 5 capsids. The insect cell-based production system for rAAV2 or rAAV1 can generate more than 4×10^4 particles of rAAV per Sf9 cell. However, the yields of rAAV5 produced with either ΔIE or Δp10 RepBac were approximately 1×10^4 to 2×10^4 vg per Sf9 cell. Rep52, or small Rep protein, has been implicated in encapsidation of the AAV genome (17). To establish a high-titer production system, we investigated the use of other serotypes of Rep52 for rAAV5 production. We replaced the type 5 Rep52 with serotype 1, 2, 3, or 4 Rep52 on the Δp10 RepBac. Figure 5A shows the results of Western blotting of Sf9 cells infected with Rep baculoviruses expressing type 5 Rep78 under the control of the Δp10 promoter and serotype 1, 2, 3, 4, or 5 Rep52 driven by the polyhedrin promoter. To generate rAAV5, Sf9 cells were coinfected with hGFPBac, VP254Bac, and a RepBac with the indicated serotype Rep52 at an MOI of 1. Sf9 cells infected with hGFPBac and VP254Bac along with RepBac producing type 1 Rep52 were processed by CsCl density centrifugation, and fractions were analyzed for capsid antigen by Western blotting (Fig. 5B). Two peaks of VP proteins were detected; the higher-buoyant-density peak, from 1.42 to 1.36 g/cm^3, presumably consists of a vector genome containing rAAV5 particles. Another peak, at 1.33 g/cm^3, represents empty capsids, indicating that type 1 Rep52 packaged serotype 5 rAAV DNA into type 5 capsids. When a RepBac that expressed only type 5 Rep78 was used, no rAAV5 particles were produced, confirming that heteroserotypic small Rep indeed packaged type 5 rAAV DNA into type 5 capsids. The cell lysate was loaded directly onto an anion-exchange column, and purified particles were investigated un-

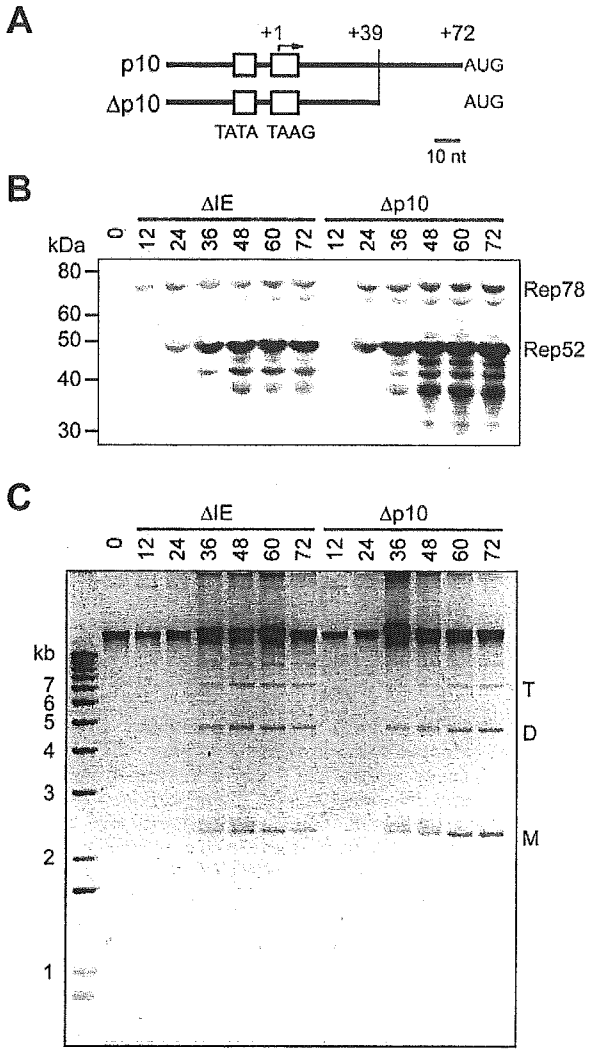

FIG. 4. (A) Map of the Δp10 promoter used for Rep78 expression. The sequence between positions +39 and +72 is deleted in the Δp10 promoter, where the T of the TAAG sequence or the transcription start site (marked with a bent arrow) is defined as +1 and the A of the p10 protein AUG codon is defined as +72. The original AUG codon for the p10 protein was mutated to ACT with pFastBac Dual (Invitrogen). The positions of the TATA box and the TAAG sequence are indicated. (B) Time course of Rep78 expression by ΔIE or Δp10 promoter. Sf9 cells were infected with a Rep baculovirus, and the cells were harvested at the times indicated (in hours) for Western analysis with a monoclonal anti-Rep antibody. (C) Replication of hGFP vector DNA in insect cells. Sf9 cells were coinfected with a Rep baculovirus and an hGFP baculovirus at 1 PFU per cell and incubated for the times indicated (in hours). Low-molecular-weight DNA was isolated, and DNA equivalent to 10^5 cells was resolved onto a 1% agarose gel. T, trimer replicative form; D, dimer; M, monomer.

der electron microscopy, showing typical rAAV particles of a diameter of 20 nm in addition to empty capsids (Fig. 5C). According to the staining pattern, approximately 30% of capsids contained vector genomes. In another experiment, rAAV5-hGFP was purified with two rounds of CsCl ultracentrifugation and the titers of rAAV5-hGFP were determined by real-time PCR using a pair of CMV-specific primers. Figure 5D summarizes the yields of rAAV5-hGFP with the use of different serotypes of small Rep. The titer of rAAV5-GFP produced with type 1, 2, 3, or 4 small Rep was 56,000 ± 3,200 (n = 4), 41,000 ± 18,900 (n = 4), 42,000 ± 7,300 (n = 3), or 39,000 ± 3,500 (n = 3) particles per Sf9 cell, respectively, while that of rAAV5-GFP produced using AAV5 Rep52 was 13,500 ± 3,200 (n = 5). The rAAV5-hGFP particles produced with the indicated serotype Rep52 were further purified by anion-exchange column chromatography, and a total of 3×10^9 vg of either rAAV5-hGFP were then fractionated by sodium dodecyl sulfate-polyacrylamide gel electrophoresis and examined by silver staining along with 293 cell-produced rAAV5-hGFP (Fig. 5E). Densitometric analysis indicated that the intensities of the VP3 bands were almost equal to one another.

Type 5 vector DNA was packaged into type 5 capsids consisting of chimeric VP1 between types 2 and 5 in the baculovirus system. To examine the possible effect of the chimeric VP1 on packaging of type 5 vector DNA with heteroserotypic Rep52, we tested the production of rAAV5-hGFP by using either Rep5/1Bac or Rep5/5Bac and VP5Bac or VP254Bac. Interestingly, the yields of rAAV5 produced with type 5 Rep52 and type 2/5 chimeric capsids were constantly lower than yields produced with other combinations (Fig. 5F). Type 1 Rep52 was capable of packaging type 5 vector DNA into type 5 capsids and type 2/5 chimeric capsids with similar levels of efficiency. Although the result was not conclusive, the presence of a type 2 VP1-unique portion might interfere with type 5 Rep52 packaging rAAV5 DNA into type 5 capsids in insect cells.

Insect cell-produced rAAV5 infects cells via an α2-3 sialic acid receptor. AAV2 capsids utilize HSPG as a primary coreceptor to infect target cells (30), whereas AAV5 capsids require α2-3 sialic acid for efficient uptake (14). rAAV5 capsids generated in Sf9 cells are composed of VP1 partially replaced with type 2 VP1. The domains involved in receptor binding are within the VP3 portion (16), and the type 2 VP1-unique portion does not appear to be involved in attachment to target cells (19). To determine whether rAAV5 chimeric capsid particles infect cells via sialic acid and not via HSPG, we performed competition experiments with receptor analogs. The results of the heparin competition study show that rAAV2-GFP failed to transduce COS cells in the presence of heparin, an analog of heparan sulfate, as expected (Fig. 6A, top panels). By contrast, rAAV5-GFP produced in 293 cells (Fig. 6A, middle panels) or insect cells (Fig. 6A, bottom panels) was able to express GFP in COS cells irrespective of the presence of heparin, suggesting that Sf9 cell-produced rAAV5-GFP did not utilize HSPG as a primary coreceptor. The number of GFP-expressing cells was counted by flow cytometry, and the percent change in transduction compared to transduction in the absence of heparin was calculated, which clearly corroborated the observation with fluorescent microscopy. We next examined whether insect cell-produced rAAV5-GFP infects cells via α2-3 sialic acid. As shown in Fig. 6B, COS cells were infected with rAAV5 generated in 293 cells (middle panels) or Sf9 cells (bottom panels) in the presence or absence of an analog of α2-3 sialic acid, 3′-SLN. The analog inhibited GFP expression in COS cells by both 293 cell- and Sf9 cell-produced rAAV5-GFP, suggesting that rAAV5-GFP produced in insect cells infected cells via α2-3 sialic acid as did 293 cell-produced rAAV5. To confirm that rAAV5-GFP derived from insect cells utilized sialic acid as a cell attachment receptor, we infected cells denuded of sialic acid by neuraminidase treatment. The

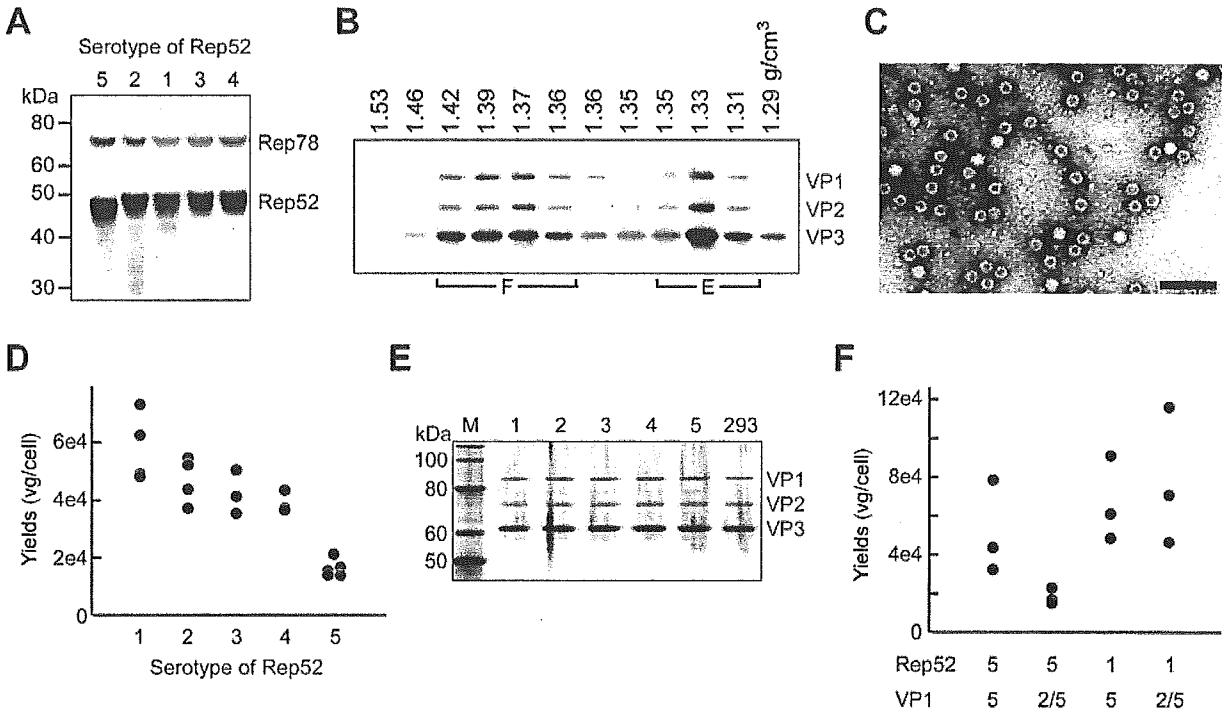

FIG. 5. (A) Western analysis of RepBacs expressing type 5 Rep78 and type 1, 2, 3, 4, or 5 Rep52 with an anti-Rep antibody. (B) Analysis of Sf9 cells coinfected with Rep, VP254, and hGFP baculoviruses by CsCl density gradient ultracentrifugation. Three days after infection, the cells were lysed and subjected to ultracentrifugation. F, filled, or containing rAAV particles; E, empty capsids. (C) Negative staining of rAAV5-hGFP particles purified with ion-exchange column chromatography alone. Particles were stained with 2% uranyl acetate. Magnification, ×100,000. Bar, 100 nm. (D) Generation of rAAV5-hGFP produced with different serotypes of Rep52. The yield of rAAV5-GFP produced with type 1, 2, 3, 4, or 5 small Rep was 56,000 ± 3,200 (n = 4), 41,000 ± 18,900 (n = 4), 42,000 ± 7,300 (n = 3), 39,000 ± 3,500 (n = 3), or 13,500 ± 3,200 (n = 5) particles per Sf9 cell, respectively. (E) Analysis of rAAV5-hGFP produced in insect cells or 293 cells by silver staining. rAAV5-hGFP (3×10^9 particles) produced with serotype 1, 2, 3, 4, or 5 and that produced in 293 cells were resolved onto a 4 to 12% NuPAGE Bis-Tris gel (Invitrogen). Lane M, molecular size markers. (F) Comparison of the yields of rAAV5-GFP produced with type 1 or type 5 Rep52 and VP5Bac or VP2/5Bac. Sf9 cells were coinfected with hGFPBac, Rep5/1Bac or Rep5/5Bac, and VP5Bac or VP254Bac at an MOI of 1 in each of three independent experiments. The rAAV5-hGFP produced was purified by two rounds of CsCl density gradient ultracentrifugation, and the genomic titer was determined by real-time PCR.

result shows that prior incubation with neuraminidase significantly inhibited the transduction of COS cells mediated by rAAV5-GFP produced in 293 cells and Sf9 cells (Fig. 6C).

Comparison of transduction efficiencies with rAAV5 in cultured cells. We next compared the efficacy of rAAV5-GFP/Neo produced in Sf9 cells to that for a mammalian-cell-produced counterpart. COS cells were infected with either Sf9-produced or 293-produced rAAV5-GFP/Neo at 1×10^5 through 1×10^2 vg per cell for 1 day, and the number of GFP-positive cells was counted by flow cytometry. As shown in Fig. 7A, both Sf9-produced and 293-produced rAAV5-GFP/Neo showed similar dose-response curves. In addition, the vector genome-to-transducing unit ratio was calculated based on the number of GFP-positive cells at 3×10^3 vg per cells. Three independently produced samples were examined, and the vector genome-to-transducing unit ratio for Sf9-produced rAAV5-GFP was $3.9 \times 10^4 \pm 1.6 \times 10^4$ (mean ± standard deviation), while the ratio for 293-produced rAAV was $3.6 \times 10^4 \pm 1.2 \times 10^4$. These results indicated that insect cell-generated rAAV5-GFP/Neo had a similar ability to transduce COS cells. Although the capsids produced in Sf9 cells contain type 2/5 chimeric VP1 and those produced in HEK293 cells were composed of original type 5 VP1, rAAV5-GFP/Neo derived from Sf9 cells and that derived from HEK293 cells did not show any significant difference in GFP expression in COS cells, suggesting that the difference in the VP1-unique portion did not impact the expression of the transgene or affect the intracellular processing of type 5 capsids in COS cells. We also compared transduction efficiencies of rAAV5-hGFP generated in Sf9 cells and rAAV5-hGFP generated in HEK293 cells. Surprisingly, the dose-response curve obtained by Sf9-produced rAAV5-hGFP shifted to the right and the number of GFP-positive cells at the dose of 3×10^3 vg per cell was five times larger than that for 293-produced rAAV5-hGFP (Fig. 7B). Since the substitution of the type 5 VP1-unique portion with the equivalent portion of type 2 did not impact the GFP expression in COS cells (Fig. 7A), we explored the rAAV genomes packaged into vector capsids. Virion DNA was isolated and analyzed on an alkaline gel. After electrophoresis, the DNA was transferred to a nylon membrane and hybridized with a ^{32}P-labeled CMV-specific probe. The GFP/Neo DNA packaged into AAV5 capsids is essentially the same in size and amount as expected (Fig. 7C). We next analyzed virion DNA isolated from rAAV5-hGFP produced with the indicated serotype Rep52 in insect cells, as well as 293-produced rAAV5-hGFP (Fig. 7D). The encapsidated hGFP DNA is present as

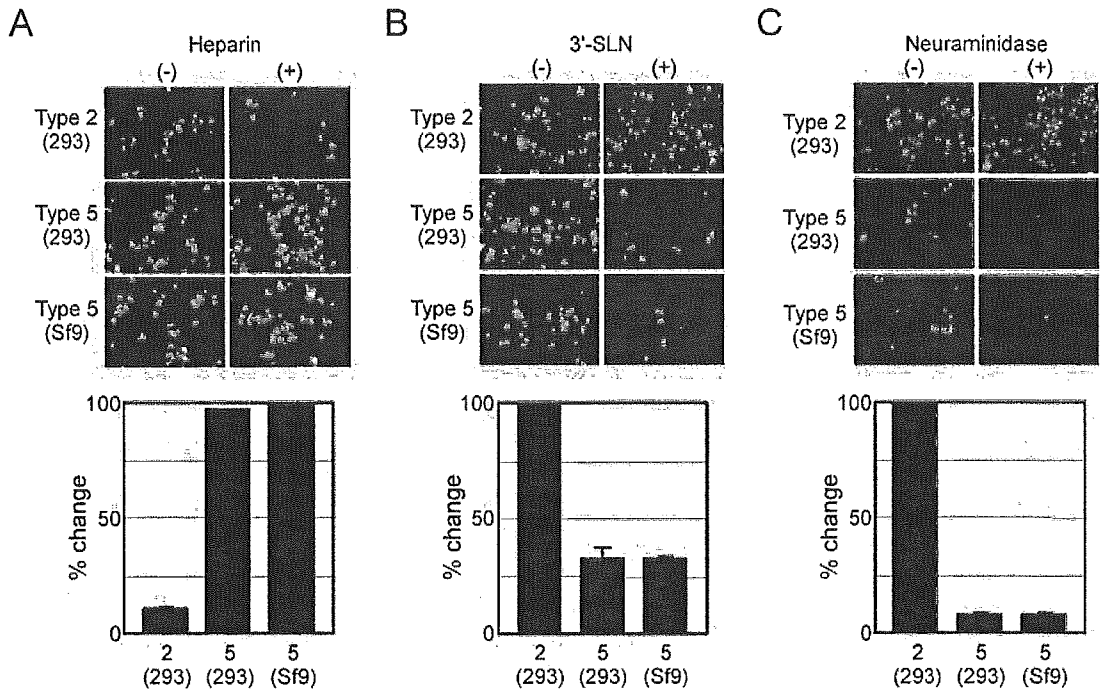

FIG. 6. (A) Heparin, an analog of HSPG, does not inhibit transduction of COS cells infected with rAAV5-GFP/Neo produced in insect cells. Cells were infected with adenovirus at 3 PFU per cell and incubated at 37°C for 2 h. After being washed with medium, the cells were infected with rAAV2-GFP/Neo produced in 293 cells at 10^4 vg per cell or rAAV5-GFP/Neo generated in 293 cells or Sf9 cells at 10^5 vg per cell in the presence or absence of 20 μg per ml of heparin in triplicate. One day after infection, the cells were observed under a fluorescent microscope. The number of GFP-positive cells was also counted by flow cytometry. Data are presented as percent change in transduction compared to transduction in the absence of heparin. (B) An analog of α2-3 sialic acid inhibits both 293 cell- and Sf9 cell-produced rAAV5-GFP/Neo. COS cells were infected with an adenovirus at 3 PFU per cell and incubated at 37°C for 2 h. After being washed with medium, the cells were infected with rAAV2-GFP/Neo at 10^4 vg per cell or rAAV5-GFP at 10^5 vg per cell for 1.5 h in the presence of 0 or 0.5 mM 3′-SLN (Sigma-Aldrich). The cells were washed twice with medium and further incubated for 1 day. The number of GFP-expressing cells was measured by flow cytometry ($n = 3$). Data are presented as percent change in transduction compared to transduction in the absence of the analog. (C) Neuraminidase treatment of COS cells inhibits transduction with rAAV5-GFP generated in 293 cells or Sf9 cells. COS cells were infected in triplicate with adenovirus at 3 PFU per cell for 1 h at 37°C, treated with 0.08 U per ml of neuraminidase (*Vibrio cholerae*, type III; Sigma-Aldrich) for 1 h, and infected with 10^5 vg per cell of rAAV5-GFP produced in 293 cells or Sf9 cells for 2 h. COS cells were similarly treated and also infected with 10^4 vg per cell of rAAV2-GFP/Neo. The infected cells were then washed twice with medium and incubated for an additional day. After incubation, the cells were observed under fluorescent microscopy and the number of GFP-positive cells was counted by flow cytometry.

two DNA species. The higher-mobility virion DNA corresponds with 2.4-kb hGFP vector DNA or a single-stranded monomer, which is confirmed by comigration with a 2.4-kb vector DNA obtained by treatment with a restriction enzyme of the hGFP vector plasmid, pSR485hGFP. The lower-mobility DNA is the same in size as the monomer RF or duplex form of hGFP DNA (Fig. 7D) isolated from Sf9 cells coinfected with RepBac and hGFPBac (Fig. 4C). The intensity of the larger virion DNA, which was quantified with an imaging analyzer, was roughly double that of shorter DNA for each rAAV5 produced in Sf9 cells. If the larger virion DNA is a monomer duplex form and thus has two CMV promoter sequences hybridizing to a CMV probe, then we estimated that the quantity of the double-stranded monomeric form was equal to that of the single-stranded monomer. The ratio of the amount of the monomer duplex form to the amount of the single-stranded monomer form in the rAAV5-hGFP virion produced in 293 cells is 1 to 3.5. AAV particles have been shown to package two copies of vector genomes that are less than 50% of the 4.8-kb AAV genome, and the packaged vector DNA appeared to be monomeric single-stranded and double-stranded RF (6). For gene expression, the single-stranded vector genome has to be converted to a double-stranded form by either second-strand synthesis (8, 9) or annealing of complementary strands (23). The monomeric duplex vector DNA, on the other hand, can function directly as a template for mRNA synthesis. Thus, the more potent gene expression mediated by rAAV5-hGFP generated in Sf9 cells is probably due to the presence of the encapsidated monomer duplex form.

Comparison of efficacies of rAAV5 in vivo. To compare the efficacies of rAAV5 produced in 293 cells and rAAV5 produced in Sf9 cells, we constructed a type 5 vector that expressed human SEAP. rAAV5 particles produced in Sf9 cells consisted of chimeric VP1 between type 2 and type 5. To eliminate the possible difference in intracellular processing of rAAV5 particles due to replacement of the type 5 VP1-unique portion with the equivalent one of type 2, we compared the in vivo activities of rAAV5 particles containing type 2/5 VP1 polypeptides produced in insect and mammalian cells. Five mice each intramuscularly received a total of 10^{11} vg of rAAV5-SEAP generated in either 293 cells or Sf9 cells, and serum SEAP levels were monitored. As shown in Fig. 8A, the expression profile of the Sf9-produced type 5 SEAP vector differed from that of the 293-produced one. The rAAV5-SEAP

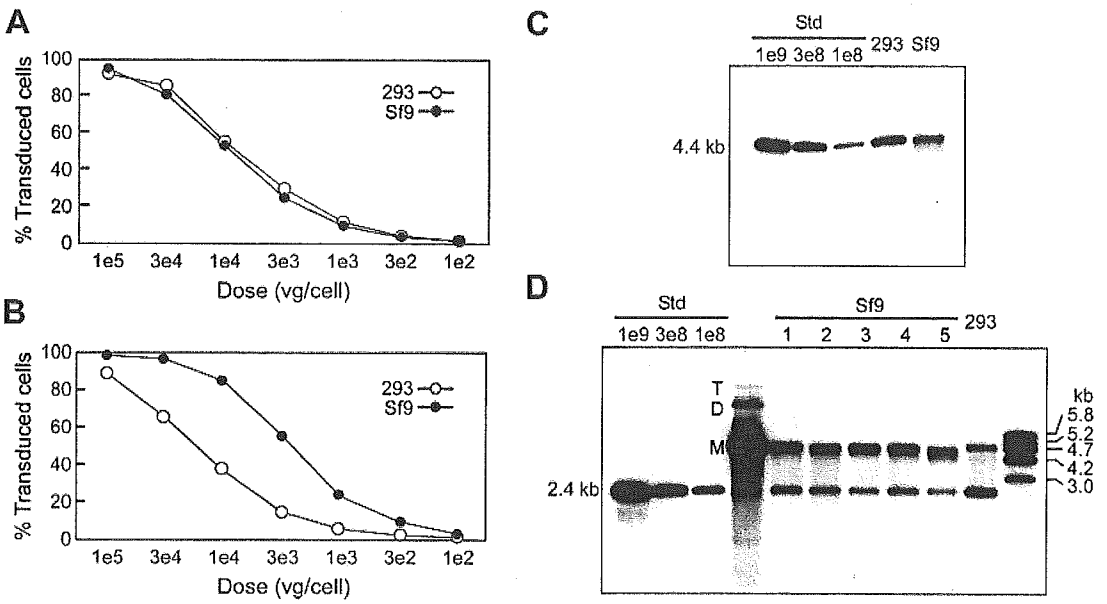

FIG. 7. Comparison of infectivities of rAAV5 produced in 293 cells and rAAV5 produced in Sf9 cells. (A) COS cells were infected with rAAV5-GFP/Neo produced in 293 cells or Sf9 cells at the doses indicated, ranging from 1×10^5 through 1×10^2 vg per cell. One day after infection, the cells were examined for GFP fluorescence by flow cytometry in triplicate. (B) COS cells were infected with rAAV5-hGFP produced in HEK293 cells or Sf9 cells at a dose of 1×10^5 through 1×10^2 vg per cell for 1 day. The number of GFP-positive cells was counted cytometrically. (C) Analysis of GFP/Neo vector virion DNA on an alkaline gel. Virion DNA was isolated from rAAV5-GFP/Neo produced in HEK293 cells or Sf9 cells by treatment with proteinase K, and samples equivalent to 3×10^8 vg were resolved onto a 0.8% alkaline gel. The DNA was then transferred to a nylon membrane and hybridized to a ^{32}P-labeled CMV-specific probe. A 4.4-kb-size copy number standard (Std) (1×10^9, 3×10^8, and 1×10^8 copies) was loaded, which was derived from the GFP/Neo vector plasmid, pSR485α, with a restriction enzyme that cut out the vector portion. (D) Alkaline agarose gel electrophoresis of virion DNA isolated from rAAV5-hGFP. Vector DNA isolated from rAAV5-hGFP particles produced with type 1, 2, 3, 4, or 5 Rep52 was analyzed along with 293-produced rAAV5-hGFP. Low-molecular-weight DNA isolated from insect cells infected with RepBac and hGFPBac (Fig. 4C) serves as a reference for monomer (M), dimer (D), and trimer (T) replicative forms.

generated in HEK293 cells showed a gradual increase in serum SEAP activity over 1 month after injection, which is a typical expression pattern by rAAV-mediated transduction. The Sf9-produced rAAV5-SEAP induced levels of SEAP activity at 1 or 2 weeks after injection that were more than 30 or 10 times higher, respectively, than those of the 293-produced rAAV5-SEAP, and the serum SEAP activity by Sf9 produced rAAV5-SEAP decreased at 4 weeks after injection. There was no significant difference between the two groups after 4 weeks following administration. We also analyzed the SEAP vector DNA on an alkaline gel (Fig. 8B). The expected size of rAAV5-SEAP vector genomes is 3.4 kb. The majority of 293-produced rAAV5-SEAP DNA is single-stranded monomer in both type 5 capsids and type 2/5 chimeric capsids. In addition to the 3.4-kb single-stranded vector genome, DNA extracted from Sf9 cell-produced rAAV5 particles contained an additional DNA of approximately 4.7 kb. One model for AAV packaging proposes that when the size of vector DNA is larger than the size of the wild-type AAV, 4.7 kb, the vector DNA is cleaved to 100% of the AAV genome during packaging into virion (6). The 4.7-kb virion DNA may be a cleaved product of duplex multimers synthesized in Sf9 cells.

DISCUSSION

Recent advances in understanding of biology of AAV and in production of rAAV have facilitated the use of rAAV as a gene transfer vector. A human clinical trial with rAAV2 expressing a coagulation factor IX has shown that intramuscular delivery of more than 10^{15} rAAV2 particles would be required for amelioration of hemophilia B (15). Currently, the widely employed method for production of rAAV is transfection of packaging cells, such as HEK293 cells, with plasmids carrying AAV and adenovirus genes. Plasmid transfection is more easily adaptable to packaging different serotype AAV vectors than establishing a packaging cell line. However, the transfection process is the limiting step in rAAV production, which requires adherent HEK293 cells on a two-dimensional surface for efficient production of rAAV.

The production of other AAV serotype-derived vectors has been described previously (26) and follows the strategy developed for rAAV2 (20). Some modifications have been reported, such as lipofection of 293 cells in suspension culture in serum-free media, which makes the handling of the cells and the purification step easier (28). However, the use of a lipid reagent for transfection may be neither cost-effective nor scalable. A recombinant herpes simplex virus harboring type 5 *rep* and *cap* genes was created to eliminate the transfection process (33), although the yields of rAAV5 were low. The baculovirus/insect cell-based rAAV5 production system presented here does not require plasmid transfection and is scalable. By extrapolation from culture volume, we expect to obtain more than 10^{14} particles of rAAV5-GFP from a 1-liter culture. This is consistent with yields of rAAV1 or rAAV2 produced in Sf9 cell cultures (20a, 31).

To produce infectious rAAV5 particles in insect cells, we

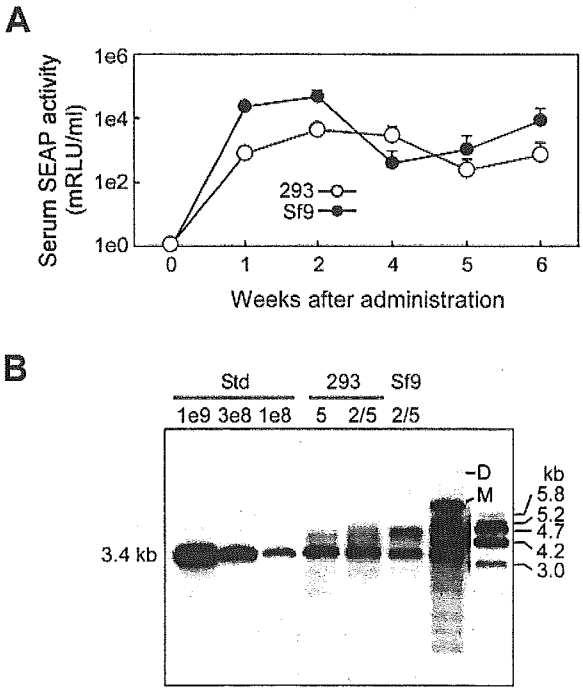

FIG. 8. (A) Serum SEAP activity following intramuscular injection of rAAV5-SEAP. Five mice each received a total of 10^{11} vg of pseudotyped rAAV5-SEAP produced in 293 cells or Sf9 cells into tibialis anterior muscles. Blood was taken at the indicated weeks after injection. The serum SEAP activity was measured by a SEAP report gene assay (Roche Diagnostics, GmbH, Penzberg, Germany). RLU, relative light units. (B) Molecular analysis of SEAP vector DNA. Vector genomes were isolated from type 5 or type 2/5 SEAP vector particles produced in HEK293 cells or from Sf9-produced rAAV5-SEAP. Extrachromosomal low-molecular-weight DNA isolated from Sf9 cells infected with RepBac and SEAPBac was also analyzed. Copies (10^9 through 10^8) of copy number standard (Std) vector DNA derived from SEAP vector plasmid, pAAVSEAP, were also loaded. M, monomer replicative form of SEAP vector genomes; D, dimer replicative form.

inserted an N-terminal portion of type 2 VP1 into the corresponding site of type 5 VP1. The N termini of VP1 polypeptides contain the phospholipase A_2 motif and are essential to viral infectivity (36). Electron microscopy indicated that the VP1-unique portion is hidden within type 2 capsids and appears on the surface of the capsids during the infectious pathway in cells (19). The VP1-unique portion is well conserved among different AAVs. Comparison of the portion among serotypes 1 through 4 and 6 revealed that one serotype is more than 80% identical to another. The type 5 VP1-unique portion is 70 to 75% identical to that of other serotypes, while the sequence alignment of VP2 or VP3 of AAV1 through AAV6 showed that type 5 is approximately 55% identical to other serotypes. The initial trial mutation of the start codon for type 5 VP1 gene to ACG failed to produce infectious rAAV5 particles due to low synthesis of VP1 polypeptide (Fig. 2C). However, the successful generation of rAAV2 particles in insect cells and the notion that the VP1-specific region is well conserved among different serotypes led us to construct a chimeric type 5 VP1 polypeptide whose N-terminal portion was partially replaced by the equivalent portion of type 2. The transduction of COS cells and mouse muscles with rAAV5 produced in insect cells clearly indicated that the chimeric VP1, VP254, could confer infectivity to it (Fig. 7 and 8).

The strategy of producing AAV "pseudotyped" vectors, typically consisting of AAV2 ITR and non-AAV2 capsids, such as AAV4 and AAV5, has been reported previously (2, 3, 26, 34). We first tested similar pseudopackaging of rAAV DNA type 2 ITRs into type 5 capsids with type 2 RepBac in insect cells. However, the yields of vector particles produced were four times lower than those reached by packaging type 5 DNA into type 5 capsids (data not shown). We also examined the production of rAAV5 by packaging type 2 AAV DNA with type 2 Rep78 and type 5 Rep52 into type 5 capsids, which also resulted in low yields of rAAV5 (data not shown). The production of type 5 vector in 293 cells by transfection with a type 5 vector plasmid and a type 5 *rep cap* plasmid usually yields more than 10^4 particles per HEK293 cell, and the production of pseudotyped type 5 vectors by using a type 2 AAV vector plasmid and type 2 *rep* and type 5 *cap* plasmid recovers 3×10^3 particles per cell (unpublished observation), an observation consistent with the production in Sf9 cells.

Using Sf9 cells, we found that Rep52 proteins of other serotypes were capable of packaging DNA with type 5 ITRs into type 5 capsids more efficiently than type 5 Rep52. Type 2 small Rep protein has been shown to package the AAV2 genome into preformed capsid with its helicase activity in collaboration with large Rep protein (7, 17). The small Rep protein associates with Rep78/68 (24) and probably specifically interacts with large Rep protein during encapsidation (7). The basis for the improved AAV packaging with non-type 5 Rep52 remains to be elucidated. To exclude the possibility that cellular proteins and/or baculovirus proteins played a major role in packaging type 5 DNA, we used a RepBac that expressed only type 5 Rep78 for production of type 5 rAAV. No rAAV5 particles were recovered from the recombinant baculovirus-infected Sf9 cells (data not shown), suggesting that the small Rep protein is absolutely required for generating rAAV5 in insect cells. As shown in Fig. 5F, the fact that the partial replacement of the VP1-unique portion with the corresponding portion of type 2, the strategy we took to generate infectious type 5 particles in insect cells, inhibited type 5 Rep52-mediated introduction of type 5 ITR genomes into type 5 capsids may only indicate the role of the type 2 VP1-unique portion as a physical barrier during packaging of rAAV genomes into capsids. We believe that under a special circumstance, such as in invertebrate cells, heteroserotypic Rep52 is superior to type 5 Rep52 in packaging rAAV DNA with type 5 ITR into type 5 capsids. It is interesting to examine whether other serotypes of Rep52 can package type 5 rAAV DNA into type 5 capsid in mammalian cells. We are currently investigating the packaging of type 5 genome into type 5 capsids with different serotypes of Rep52 in HEK293 cells.

The majority of the vector genome of rAAV5 produced in HEK293 cells in the present study is in single-stranded monomeric form, irrespective of the size of the vector genome (Fig. 7C and D and 8B). However, when the size of vector DNA is shorter than the size of the wild-type AAV genome, insect cells tend to package longer, 4.7-kb DNA into type 5 capsids. The 4.7-kb longer virion DNA in Sf9-produced rAAV5 appears to be a cleavage product of multimers of replicated vector genomes. If the size of a multimer is within the packaging limit,

it is efficiently introduced into AAV capsids. If a multimer is larger than 4.8 kb in size, a partially truncated multimer is packaged into AAV capsids in insect cells (6). Sequencing of 4.7-kb DNA packaged into virions will be a key to disclosing the difference between packaging of vector DNA into capsids in HEK293 cells and insect cells. The difference in packaged virion DNA between rAAV5 produced in human cells and in insect cells provides important information on designing vector DNA for production of rAAV5 in insect cells.

In summary, we developed a new method for production of rAAV5 in insect cells, which offers a better alternative to the existing production methods of rAAV5, although the vector genomes packaged into capsids differ in size from rAAV5 produced in HEK293 cells. The robust generation in suspension culture will facilitate the use of type 5 rAAV not only for basic studies but also for clinical studies.

ACKNOWLEDGMENTS

This work was supported in part by grants from the Ministry of Health, Welfare, and Labor of Japan and Grants-in-Aid for Scientific Research from the Ministry of Education, Science, Sports, and Technology of Japan, and High-Tech Research Center Project for private universities (matching-fund subsidy from the Ministry of Education, Science, Sports, and Technology of Japan). This research was also supported in part by the Intramural Research Program of the NHLBI, NIH.

REFERENCES

1. **Balsinde, J., M. A. Balboa, P. A. Insel, and E. A. Dennis.** 1999. Regulation and inhibition of phospholipase A2. Annu. Rev. Pharmacol. Toxicol. **39:**175–189.
2. **Chiorini, J. A., F. Kim, L. Yang, and R. M. Kotin.** 1999. Cloning and characterization of adeno-associated virus type 5. J. Virol. **73:**1309–1319.
3. **Chiorini, J. A., L. Yang, Y. Liu, B. Safer, and R. M. Kotin.** 1997. Cloning of adeno-associated virus type 4 (AAV4) and generation of recombinant AAV4 particles. J. Virol. **71:**6823–6833.
4. **Conway, J. E., C. M. Rhys, I. Zolotukhin, S. Zolotukhin, N. Muzyczka, G. S. Hayward, and B. J. Byrne.** 1999. High-titer recombinant adeno-associated virus production utilizing a recombinant herpes simplex virus type I vector expressing AAV-2 Rep and Cap. Gene Ther. **6:**986–993.
5. **Davidson, B. L., C. S. Stein, J. A. Heth, I. Martins, R. M. Kotin, T. A. Derksen, J. Zabner, A. Ghodsi, and J. A. Chiorini.** 2000. Recombinant adeno-associated virus type 2, 4, and 5 vectors: transduction of variant cell types and regions in the mammalian central nervous system. Proc. Natl. Acad. Sci. USA **97:**3428–3432.
6. **Dong, J. Y., P. D. Fan, and R. A. Frizzell.** 1996. Quantitative analysis of the packaging capacity of recombinant adeno-associated virus. Hum. Gene Ther. **7:**2101–2112.
7. **Dubielzig, R., J. A. King, S. Weger, A. Kern, and J. A. Kleinschmidt.** 1999. Adeno-associated virus type 2 protein interactions: formation of pre-encapsidation complexes. J. Virol. **73:**8989–8998.
8. **Ferrari, F. K., T. Samulski, T. Shenk, and R. J. Samulski.** 1996. Second-strand synthesis is a rate-limiting step for efficient transduction by recombinant adeno-associated virus vectors. J. Virol. **70:**3227–3234.
9. **Fisher, K. J., G. P. Gao, M. D. Weitzman, R. DeMatteo, J. F. Burda, and J. M. Wilson.** 1996. Transduction with recombinant adeno-associated virus for gene therapy is limited by leading-strand synthesis. J. Virol. **70:**520–532.
10. **Gao, G. P., G. Qu, L. Z. Faust, R. K. Engdahl, W. Xiao, J. V. Hughes, P. W. Zoltick, and J. M. Wilson.** 1998. High-titer adeno-associated viral vectors from a Rep/Cap cell line and hybrid shuttle virus. Hum. Gene Ther. **9:**2353–2362.
11. **Grunert, S., and R. J. Jackson.** 1994. The immediate downstream codon strongly influences the efficiency of utilization of eukaryotic translation initiation codons. EMBO J. **13:**3618–3630.
12. **Hirt, B.** 1967. Selective extraction of polyoma DNA from infected mouse cell cultures. J. Mol. Biol. **26:**365–369.
13. **Hölscher, C., J. A. Kleinschmidt, and A. Bürkle.** 1995. High-level expression of adeno-associated virus (AAV) Rep78 or Rep68 protein is sufficient for infectious-particle formation by a *rep*-negative AAV mutant. J. Virol. **69:**6880–6885.
14. **Kaludov, N., K. E. Brown, R. W. Walters, J. Zabner, and J. A. Chiorini.** 2001. Adeno-associated virus serotype 4 (AAV4) and AAV5 both require sialic acid binding for hemagglutination and efficient transduction but differ in sialic acid linkage specificity. J. Virol. **75:**6884–6893.
15. **Kay, M. A., C. S. Manno, M. V. Ragni, P. J. Larson, L. B. Couto, A. McClelland, B. Glader, A. J. Chew, S. J. Tai, R. W. Herzog, V. Arruda, F. Johnson, C. Scallan, E. Skarsgard, A. W. Flake, and K. A. High.** 2000. Evidence for gene transfer and expression of factor IX in haemophilia B patients treated with an AAV vector. Nat. Genet. **24:**257–261.
16. **Kern, A., K. Schmidt, C. Leder, O. J. Muller, C. E. Wobus, K. Bettinger, C. W. Von der Lieth, J. A. King, and J. A. Kleinschmidt.** 2003. Identification of a heparin-binding motif on adeno-associated virus type 2 capsids. J. Virol. **77:**11072–11081.
17. **King, J. A., R. Dubielzig, D. Grimm, and J. A. Kleinschmidt.** 2001. DNA helicase-mediated packaging of adeno-associated virus type 2 genomes into preformed capsids. EMBO J. **20:**3282–3291.
18. **Kozak, M.** 1986. Point mutations define a sequence flanking the AUG initiator codon that modulates translation by eukaryotic ribosomes. Cell **44:**283–292.
19. **Kronenberg, S., B. Bottcher, C. W. von der Lieth, S. Bleker, and J. A. Kleinschmidt.** 2005. A conformational change in the adeno-associated virus type 2 capsid leads to the exposure of hidden VP1 N termini. J. Virol. **79:**5296–5303.
20. **Matsushita, T., S. Elliger, C. Elliger, G. Podsakoff, L. Villarreal, G. J. Kurtzman, Y. Iwaki, and P. Colosi.** 1998. Adeno-associated virus vectors can be efficiently produced without helper virus. Gene Ther. **5:**938–945.

20a. **Meghrous, J., M. G. Aucoin, D. Jacob, P. S. Chahal, N. Arcand, and A. A. Kamen.** 2005. Production of recombinant adeno-associated viral vectors using a baculovirus/insect cell suspension culture system: from shake flasks to a 20-L bioreactor. Biotechol. Prog. **21:**154–160.

21. **Murakami, M., and I. Kudo.** 2004. Secretory phospholipase A2. Biol. Pharm. Bull. **27:**1158–1164.
22. **Muramatsu, S., H. Mizukami, N. S. Young, and K. E. Brown.** 1996. Nucleotide sequencing and generation of an infectious clone of adeno-associated virus 3. Virology **221:**208–217.
23. **Nakai, H., T. A. Storm, and M. A. Kay.** 2000. Recruitment of single-stranded recombinant adeno-associated virus vector genomes and intermolecular recombination are responsible for stable transduction of liver in vivo. J. Virol. **74:**9451–9463.
24. **Pereira, D. J., D. M. McCarty, and N. Muzyczka.** 1997. The adeno-associated virus (AAV) Rep protein acts as both a repressor and an activator to regulate AAV transcription during a productive infection. J. Virol. **71:**1079–1088.
25. **Qiu, J., R. Nayak, G. E. Tullis, and D. J. Pintel.** 2002. Characterization of the transcription profile of adeno-associated virus type 5 reveals a number of unique features compared to previously characterized adeno-associated viruses. J. Virol. **76:**12435–12447.
26. **Rabinowitz, J. E., F. Rolling, C. Li, H. Conrath, W. Xiao, X. Xiao, and R. J. Samulski.** 2002. Cross-packaging of a single adeno-associated virus (AAV) type 2 vector genome into multiple AAV serotypes enables transduction with broad specificity. J. Virol. **76:**791–801.
27. **Smith, R. H., S. A. Afione, and R. M. Kotin.** 2002. Transposase-mediated construction of an integrated adeno-associated virus type 5 helper plasmid. BioTechniques **33:**204–206, 208, 210–211.
28. **Smith, R. H., C. Ding, and R. M. Kotin.** 2003. Serum-free production and column purification of adeno-associated virus type 5. J. Virol. Methods **114:**115–124.
29. **Snyder, R. O.** 1999. Adeno-associated virus-mediated gene delivery. J. Gene Med. **1:**166–175.
30. **Summerford, C., and R. J. Samulski.** 1998. Membrane-associated heparan sulfate proteoglycan is a receptor for adeno-associated virus type 2 virions. J. Virol. **72:**1438–1445.
31. **Urabe, M., C. Ding, and R. M. Kotin.** 2002. Insect cells as a factory to produce adeno-associated virus type 2 vectors. Hum. Gene Ther. **13:**1935–1943.
32. **Weyer, U., and R. D. Possee.** 1989. Analysis of the promoter of the Autographa californica nuclear polyhedrosis virus p10 gene. J. Gen. Virol. **70:**203–208.
33. **Wustner, J. T., S. Arnold, M. Lock, J. C. Richardson, V. B. Himes, G. Kurtzman, and R. W. Peluso.** 2002. Production of recombinant adeno-associated type 5 (rAAV5) vectors using recombinant herpes simplex viruses containing *rep* and *cap*. Mol. Ther. **6:**510–518.
34. **Yan, Z., R. Zak, G. W. Luxton, T. C. Ritchie, U. Bantel-Schaal, and J. F. Engelhardt.** 2002. Ubiquitination of both adeno-associated virus type 2 and 5 capsid proteins affects the transduction efficiency of recombinant vectors. J. Virol. **76:**2043–2053.
35. **Yang, S., and L. K. Miller.** 1999. Activation of baculovirus very late promoters by interaction with very late factor 1. J. Virol. **73:**3404–3409.
36. **Zadori, Z., J. Szelei, M. C. Lacoste, Y. Li, S. Gariepy, P. Raymond, M. Allaire, I. R. Nabi, and P. Tijssen.** 2001. A viral phospholipase A2 is required for parvovirus infectivity. Dev. Cell **1:**291–302.

ARTICLE

doi:10.1016/j.ymthe.2005.08.009

Viral-Mediated Temporally Controlled Dopamine Production in a Rat Model of Parkinson Disease

Xiao-gang Li,[1,2] Takashi Okada,[2] Mika Kodera,[1] Yuko Nara,[1] Naomi Takino,[1] Chieko Muramatsu,[1] Kunihiko Ikeguchi,[1] Fumi Urano,[3] Hiroshi Ichinose,[3] Daniel Metzger,[4] Pierre Chambon,[4] Imaharu Nakano,[1] Keiya Ozawa,[2,*] and Shin-ichi Muramatsu[1,†]

[1]*Division of Neurology, Department of Medicine, and* [2]*Divison of Genetic Therapeutics, Center for Molecular Medicine, Jichi Medical School, Tochigi 329-0498, Japan*

[3]*Department of Life Science, Tokyo Institute of Technology, Kanagawa 226-8501, Japan*

[4]*Institut de Génétique et de Biologie Moléculaire et Cellulaire, Centre National de la Recherche Scientifique, Institut National de la Santé et de la Recherche Médicale, Université Louis Pasteur, Collège de France, and Institut Clinique de la Souris, 67404 Illkirch Cedex, France*

**To whom correspondence and reprint requests should be addressed at the Division of Genetic Therapeutics, Center for Molecular Medicine, Jichi Medical School, 3311-1 Yakushiji, Minamikawachi, Tochigi 329-0498, Japan. Fax: +81 285 44 8675. E-mail: kozawa@ms.jichi.ac.jp.*

†To whom correspondence and reprint requests should be addressed at the Division of Neurology, Department of Medicine, Jichi Medical School, 3311-1 Yakushiji, Minamikawachi, Tochigi 329-0498, Japan. Fax: +81 285 44 5118. E-mail: muramats@ms.jichi.ac.jp.

Available online 22 September 2005

Regulation of gene expression is necessary to avoid possible adverse effects of gene therapy due to excess synthesis of transgene products. To reduce transgene expression, we developed a viral vector-mediated somatic regulation system using inducible Cre recombinase. A recombinant adeno-associated virus (AAV) vector expressing Cre recombinase fused to a mutated ligand-binding domain of the estrogen receptor α (CreER^{T2}) was delivered along with AAV vectors expressing dopamine-synthesizing enzymes to rats of a Parkinson disease model. Treatment with 4-hydroxytamoxifen, a synthetic estrogen receptor modulator, activated Cre recombinase within the transduced neurons and induced selective excision of the tyrosine hydroxylase (TH) coding sequence flanked by loxP sites, leading to a reduction in transgene-mediated dopamine synthesis. Using this strategy, aromatic L-amino acid decarboxylase (AADC) activity was retained so that L-3,4-dihydroxyphenylalanine (L-dopa), a substrate for AADC, could be converted to dopamine in the striatum and the therapeutic effects of L-dopa preserved, even after reduction of TH expression in the case of dopamine overproduction. Our data demonstrate that viral vector-mediated inducible Cre recombinase can serve as an *in vivo* molecular switch, allowing spatial and temporal control of transgene expression, thereby potentially increasing the safety of gene therapy.

Key Words: adeno-associated virus, gene therapy, gene regulation, tamoxifen, Cre recombinase, Parkinson disease, dopamine

INTRODUCTION

Advances in gene transfer methods, in particular the development of improved viral vectors, have expanded the potential of gene therapy to treat a wide range of genetic and acquired diseases. Efficient and long-term expression of therapeutic genes within the central nervous system has been demonstrated in preclinical studies aimed at treating neurodegenerative disorders, including Parkinson disease (PD) [1,2]. PD is a progressive movement disorder characterized by selective degeneration of dopaminergic neurons within the substantia nigra, which project to the striatum. As the dopamine content of the striatum decreases severely, its replacement becomes an important strategy to alleviate motor impairment of the disease. One such strategy is gene therapy to restore the local production of dopamine. Recombinant adeno-associated virus (AAV) vector-mediated gene transfer of dopamine-synthesizing enzymes, such as tyrosine hydroxylase (TH) and guanosine triphosphate cyclohydrolase I (GCH), with or without aromatic L-amino acid decarboxylase (AADC), has induced behavioral recovery in animal models of PD [3–5]. Before clinical trials examining this therapy can commence, however, it is desirable to have a mechanism by which

1525-0016/$30.00

dopamine synthesis can be controlled by regulation of gene expression.

Methods utilizing the properties of bacteriophage P1 site-specific Cre recombinase have been developed in recent years as a means of generating somatic mutations [6]. Regulation of Cre recombinase activity, achieved by fusing Cre with mutated hormone-binding domains of various steroid receptors, has been used in various transgenic applications [7,8]. A chimeric protein known as CreER^{T2}, obtained by fusing Cre to a mutated ligand binding domain of the human estrogen receptor α, is particularly useful. Cell-specific expression of CreER^{T2} in transgenic mice allows efficient tamoxifen-dependent Cre-mediated recombination at loci flanked by loxP sites, without background activity [9]. In the present study, we demonstrate that stereotaxic injection of recombinant AAV vectors expressing dopamine-synthesizing enzymes and CreER^{T2} enables spatiotemporal control of dopamine levels within the brains of rats of a PD model. Our results indicate that these vectors may have a number of applications in gene therapy.

RESULTS

Viral-Mediated Temporally Controlled Cre-Mediated Recombination

We generated AAV vectors expressing either Cre recombinase containing a nuclear localization signal (AAV-Cre) or tamoxifen-dependent Cre recombinase (AAV-CreER^{T2}). To engineer a reporter system, we designed an AAV-EGFP/Red vector to express a destabilized variant of red fluorescent protein (DsRed-Express DR) only after Cre-mediated recombination of a loxP-flanked DNA segment encoding a destabilized, red-shifted variant of green fluorescent protein (d2EGFP) (Fig. 1A). To determine the efficacy of viral-mediated recombination, we infected HEK293 cells with AAV-EGFP/Red and either AAV-Cre or AAV-CreER^{T2} (Fig. 1B). Co-infection of AAV-Cre and AAV-EGFP/Red resulted in expression of DsRed-Express-DR, while only d2EGFP was expressed in control cells infected with AAV-EGFP/Red alone. Co-infection with the reporter vector and AAV-CreER^{T2} induced DsRed-Express-DR expression in almost all 4-hydroxytamoxifen (4-OHT)-treated cells. Although we detected slight background expression of DsRed-Express-DR in the absence of 4-OHT, we observed only a limited number of these cells (<1%), indicating that CreER^{T2} activity is tightly regulated in these virally transduced cells. To test the potential use of AAV-CreER^{T2} *in vivo*, we used stereotaxic injections to deliver AAV-CreER^{T2} into the brains of reporter mice [10]. These mice were engineered to express a red-shifted variant of the wild-type green fluorescent protein (EGFP) only after Cre-mediated excision of a loxP DNA fragment. After 5 consecutive days of 4-OHT treatment (1 mg by intraperitoneal injection), we observed numerous EGFP-expressing cells in AAV-injected brains, all of which coexpressed Cre recombinase (Fig. 1C). In the absence of treatment with 4-OHT, only a few cells (<0.1% of Cre-positive cells) expressed EGFP in the vicinity of AAV-CreER^{T2}-injected sites (data not shown). These data indicate that floxed DNA segments are efficiently excised *in vivo* by combining AAV-CreER^{T2} injection with 4-OHT treatment.

Temporally Controlled Reduction of Dopamine Synthesis

We generated AAV vectors expressing each of the three dopamine-synthesizing enzymes (TH, AADC, and GCH). In the TH-expressing vector, two loxP sites flanked the TH coding sequence (AAV-floxed TH). We infected HEK293 cells with these dopamine-synthesizing vectors (AAV-floxed TH, AAV-AADC, and AAV-GCH) in combination

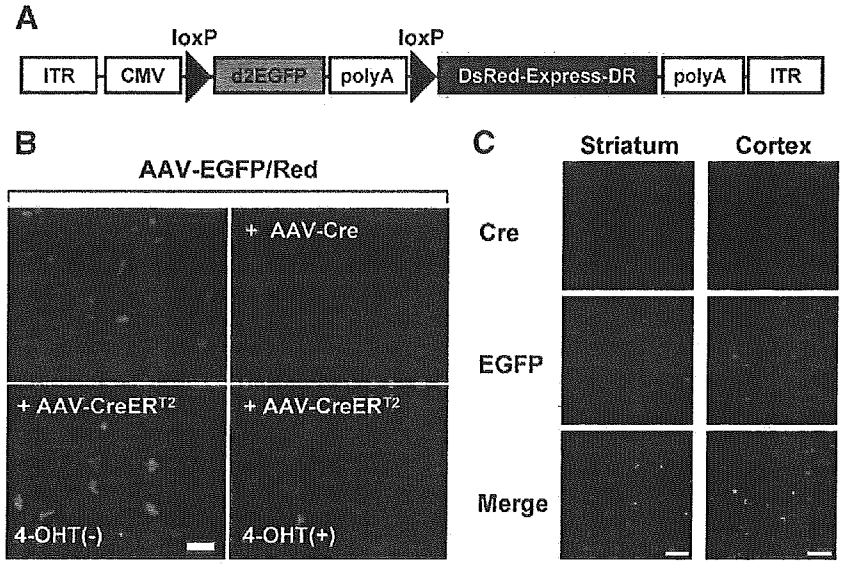

FIG. 1. Viral vector-mediated Cre-dependent floxed DNA excision. (A) Illustration of the AAV-EGFP/Red vector construct. A DsRed-Express-DR marker was placed downstream of the d2EGFP marker with a SV40 poly(A) sequence flanked by loxP sites. ITR, inverted terminal repeat; CMV, human cytomegalovirus immediate-early promoter followed by the first intron of human growth hormone. (B) 4-OHT-induced Cre-dependent recombination. HEK293 cells were infected with AAV-EGFP/Red and either AAV-Cre or AAV-CreER^{T2}. 4-OHT was added to the medium 5 h after infection. Fluorescence was observed 48 h after infection. Bar, 40 μm. (C) EGFP expression in the AAV-CreER^{T2}-injected striatum and cortex of transgenic mice. 4-OHT (1 mg) was administered intraperitoneally 1 week after vector injection every day for 5 days until the mice were killed. In these mice, the stop fragment was flanked by loxP sites and placed between the EGFP sequence and the *Gt(ROSA)26Sor* promoter. Bar, 40 μm.

doi:10.1016/j.ymthe.2005.08.009

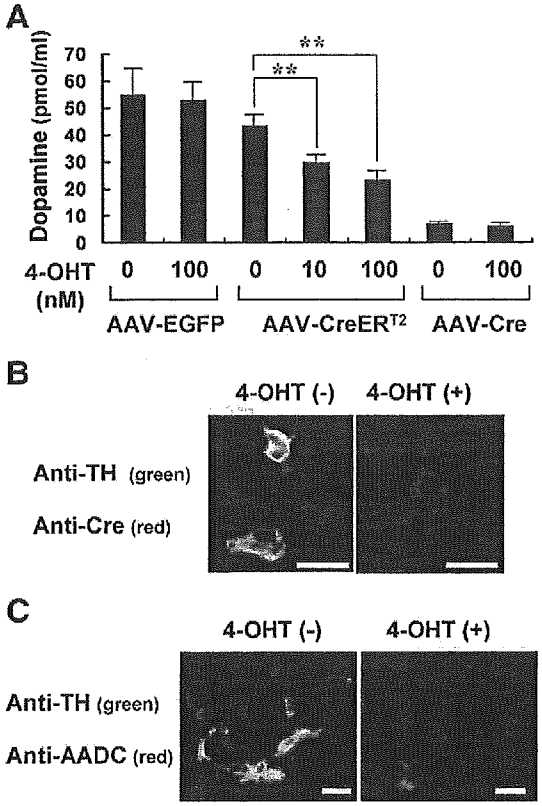

FIG. 2. Reduced dopamine synthesis after 4-OHT-induced ablation of a floxed TH transgene. HEK293 cells were infected with dopamine-synthesizing vectors (AAV-floxed TH, AAV-AADC, and AAV-GCH) in combination with AAV-CreER^{T2} or control vectors. (A) Dopamine content in the culture medium was significantly reduced in the presence of 4-OHT. $^{**}P < 0.01$, $n = 4$. (B) TH (green) and CreER^{T2} (red) immunocytochemistry was performed 48 h after vector infection. Yellow fluorescence in the merged image indicates colocalization. In the presence of 4-OHT, CreER^{T2} translocated to the nucleus. TH was not expressed in cells positive for nuclear CreER^{T2}. Bar, 20 μm. (C) TH (green) and AADC (red) immunocytochemistry. Note the reduced number of TH-positive cells in the presence of 4-OHT. Bar, 20 μm.

with AAV-CreER^{T2} or control vectors. We found that treatment with 4-OHT significantly reduced dopamine synthesis (Fig. 2A). Immunocytochemistry demonstrated coexpression of TH and CreER^{T2} in the cytoplasm in the absence of 4-OHT and an absence of TH expression when CreER^{T2} was translocated into the nucleus in the presence of 4-OHT (Fig. 2B). The expression of AADC was not reduced by the presence of 4-OHT (Fig. 2C). Dual labeling showed that more than 80% of the TH-immunoreactive (TH-IR) cells were also positive for AADC (251 of 300) and Cre (242 of 300) in the absence of 4-OHT-treatment.

Reduction of Dopamine Production in a Rat Model

We next tested whether the vector-mediated Cre-dependent regulation of transgene expression observed in culture could be extended to animal models. We obtained hemiparkinsonian rats by injecting a selective neurotoxin, 6-hydroxydopamine (6-OHDA), into the left medial forebrain bundle. The animals then received a mixture of AAV-CreER^{T2}, AAV-floxed TH, AAV-AADC, and AAV-GCH into their lesioned striatum, after which two-thirds were further treated with 4-OHT (4 mg/kg by intraperitoneal injection for 5 days) during the course of experimentation. Control rats were injected with AAV-LacZ alone or with AAV-Cre plus AAV-floxed TH, AAV-AADC, and AAV-GCH. To evaluate abnormal motor functions associated with depletion of dopamine in the striatum, we repeated quantification of apomorphine-induced rotation, as well

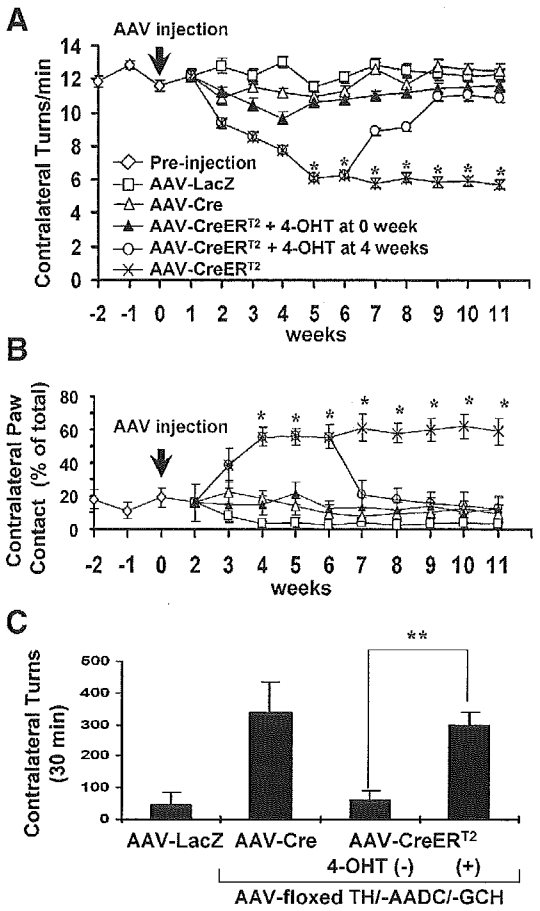

FIG. 3. Temporal control of dopamine synthesis in a rat model of PD transduced with AAV vectors. Sixty hemiparkinsonian rats were generated by 6-OHDA injection. Thirty-six received a mixture of AAV-CreER^{T2}, AAV-floxed TH, AAV-AADC, and AAV-GCH, after which they were divided into three groups of 12. Two of the groups were treated with 4-OHT (4 mg/kg by intraperitoneal injection for 5 days), at the same time or 4 weeks after vector injection. Control PD rats were injected with AAV-LacZ alone ($n = 12$) or AAV-Cre ($n = 12$), instead of AAV-CreER^{T2} with AAV-floxed TH, AAV-AADC, and AAV-GCH. (A) The total number of complete body turns induced by apomorphine was counted for each rat, and (B) spontaneous limb use was scored using the cylinder test. $^{*}P < 0.05$. (C) Efficient conversion of L-dopa to dopamine by AADC. L-Dopa (5 mg/kg) was administered to 4-OHT-treated rats and AAV-Cre-injected rats. Contralateral turning in response to L-dopa was counted for 30 min. $^{**}P < 0.01$. Legend symbols are as shown in A and B.

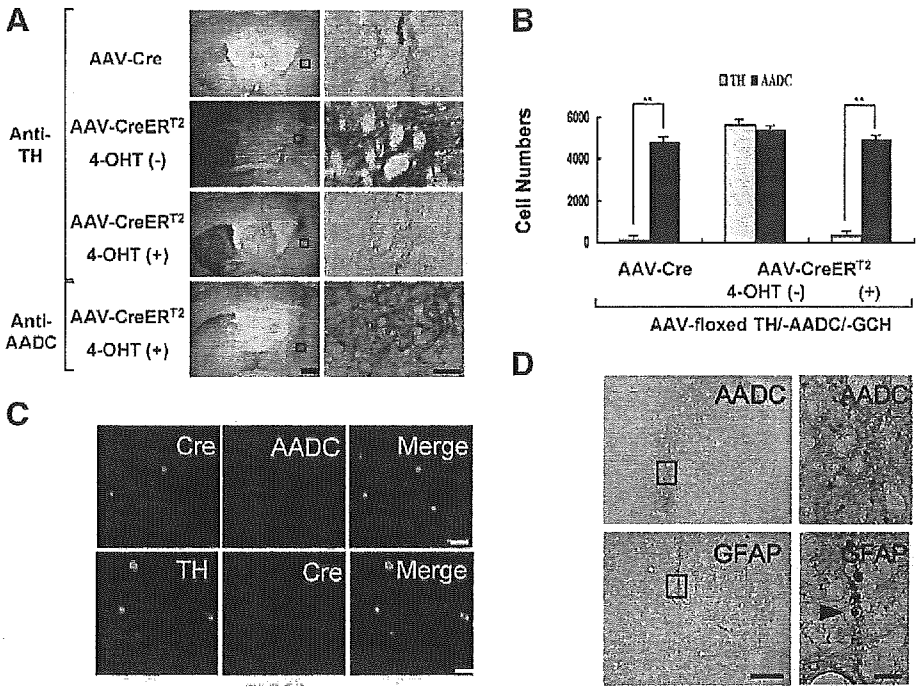

FIG. 4. Selective ablation of the TH transgene induced by treatment with 4-OHT. (A) Immunohistochemical staining for TH or AADC in the brains of 6-OHDA-lesioned rats 12 weeks after stereotaxic injection of AAV-Cre or AAV-CreER^{T2}, with or without 4-OHT treatment. AAV vectors were injected into the lesioned side of the striatum (right side of the photos). High-power-magnified images of the vector injection sites (squares in the left column) are shown in the right column. Representative photographs are also shown. Bar, 1.5 mm (left column), 100 μm (right column). (B) Number of immunoreactive (IR) cells against TH or AADC in the multiple AAV vector-injected striatum. The number of cells in 11 sections per rat (n = 3 for each group) was counted. The numbers of TH-IR cells and AADC-IR cells in AAV-CreER^{T2}-injected rats given 4-OHT 0 or 4 weeks after vector injection were indistinguishable and the results pooled for comparison with other groups. $^{**}P < 0.01$. (C) Efficient cotransduction of AAV vectors, as determined by dual immunofluorescence staining of the 6-OHDA-lesioned striatum. The majority of Cre-IR cells were also positive for TH and AADC. Bar, 20 μm. (D) Parallel striatal sections immunostained for glial fibrillary acidic protein (GFAP) or AADC. Striatal cells were transduced without obvious reactive astrocytosis. Residual hemosiderin was observed along the needle tract. On the right are magnified views of the boxes on the left. Bars: 0.5 mm, left; 50 μm, right.

as the cylinder test, weekly until the rats were killed. In the absence of 4-OHT, we observed behavioral recovery in rats that received both AAV-CreER^{T2} and AAV vectors expressing dopamine-synthesizing enzymes. Following 4-OHT treatment, these rats regressed, demonstrating impaired behavior (Figs. 3A and 3B). No recovery occurred in AAV-CreER^{T2}-injected rats treated with 4-OHT at the same time as vector injection or in AAV-Cre- or AAV-LacZ-injected rats. Contralateral turning in response to L-3,4-dihydroxyphenylalanine (L-dopa, 5 mg/kg) was not significantly reduced in 4-OHT-treated rats or AAV-Cre injected rats, indicating efficient conversion of L-dopa to dopamine in the striatum due to preservation of AADC activity (Fig. 3C).

Immunohistochemistry showed fewer TH-IR cells in rats that received AAV-Cre or AAV-CreER^{T2} plus 4-OHT, compared to injected rats not treated with 4-OHT (Figs. 4A and 4B). The numbers of AADC-immunoreactive cells,

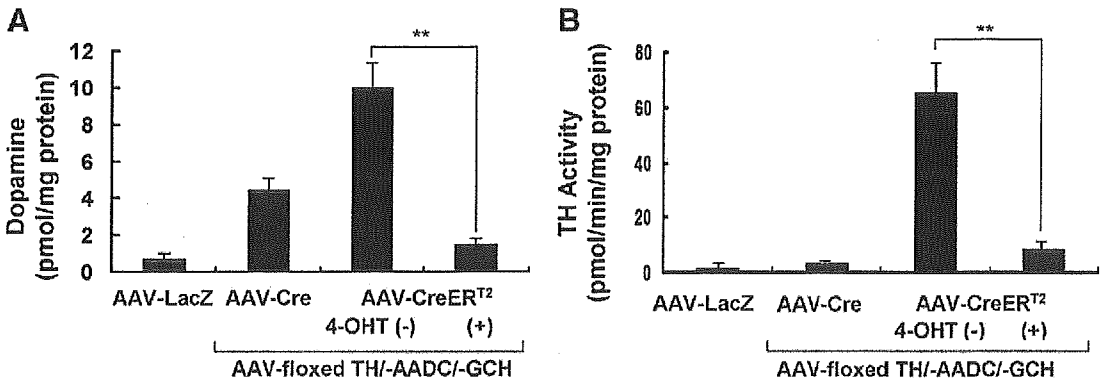

FIG. 5. Reduction of dopamine synthesis in 4-OHT-treated rats. Significantly less (A) dopamine content and (B) TH activity were observed in the lesioned striatum of 4-OHT-treated rats 12 weeks after vector injection, compared to 4-OHT-untreated rats. $^{**}P < 0.01$, n = 4.

doi:10.1016/j.ymthe.2005.08.009

however, did not differ significantly between 4-OHT-treated and untreated rats. We roughly estimated the number of transduced cells in the striatum at 5×10^4 based on cell counts performed on the tissue sections. This efficiency of transduction is sufficient to parallel the functional effects on behavior observed in other studies [3,5,11]. Double-labeling with both anti-Cre and anti-TH antibodies, or with anti-Cre and anti-AADC antibodies, showed that more than 80% of Cre-immunoreactive cells were also positive for TH (164 of 200) and AADC (176 of 200) in three 4-OHT-untreated rats (Fig. 4C). Immunostaining for glial fibrillary acidic protein (GFAP) or AADC in parallel sections demonstrated transduction of striatal cells without obvious reactive astrocytosis (Fig. 4D). Dopamine content (Fig. 5A) and TH activity (Fig. 5B) within the lesioned striatum were significantly lower in 4-OHT-treated compared to untreated rats. Dopamine levels in the transduced striatum in the 4-OHT-treated and untreated rats were 0.66 and 4.3%, respectively, those of the unlesioned striatum. Unlike primary dopamine in the nigrostriatal system, which is stored in synaptic vesicles, genetically produced dopamine in the lesioned striatum might be readily metabolized without storage. Since the dopamine level in the lesioned side of AAV-LacZ-injected rats was much lower (0.3%), a 10-fold increase in dopamine level after triple transduction with TH, AADC, and GCH genes caused a remarkable therapeutic effect. Average TH activity, measured in terms of L-dopa production (pmol/min/mg protein), reached 51.6% that of the normal striatum (65.9 ± 11.0 versus 127.7 ± 3.7) in rats transduced with dopamine-synthesizing enzymes. In 4-OHT-treated rats, TH activity fell to 10.8% of normal (13.8 ± 4.1).

Discussion

Our results show efficient viral vector-mediated delivery of tamoxifen-dependent $CreER^{T2}$ recombinase into rodent brains and that transgenic floxed sequences can be deleted in a temporally controlled manner. In a rat model of PD, recombinant AAV vector-mediated delivery of $CreER^{T2}$ into the striatum enabled 4-OHT-induced excision of a floxed TH transgene, resulting in reduced virally mediated dopamine synthesis. We targeted TH, a rate-limiting enzyme for dopamine biosynthesis that converts dietary L-tyrosine to L-dopa. Using this strategy, AADC activity was retained so that L-dopa, a substrate for AADC capable of crossing the blood–brain barrier, could be converted to dopamine in the striatum. Thus, in clinical situations, the therapeutic effects of orally administered L-dopa would likely be preserved, even after 4-OHT treatment to reduce TH expression in cases of dopamine overproduction [11]. Although transduction with AADC alone, in combination with oral administration of L-dopa, might not achieve continuous delivery of L-dopa, in contrast to that which could potentially be achieved with triple transduction of TH, AADC, and GCH, dopamine production could be regulated by altering the dose of L-dopa, thereby providing a safer option for gene therapy. We previously demonstrated that dopamine synthesis was enhanced (greater than fivefold) after systemic administration of L-dopa in AAV-TH/-AADC/-GCH-injected striatum in the primate model of PD using *in vivo* dialysis [4]. A phase I clinical trial involving gene transfer of AADC alone is currently under way.

AAV vectors are powerful tools by which to deliver therapeutic genes into the mammalian brain. Many striatal neurons of rodents and nonhuman primates are transduced with AAV vectors via stereotaxic injection, and long-term gene expression has been achieved without substantial toxicity or immune response [2,12]. AAV vectors have safety advantages over other viral vectors when it comes to *in vivo* gene delivery, since they are derived from nonpathogenic wild-type viruses. Moreover, most recombinant AAVs are present in cells as episomes, thus reducing the probability of insertional activation of oncogenes, compared to retroviruses, which integrate into host chromosomes [13]. Although it is difficult to use a single AAV vector for multiple gene transfer due to its limited packaging capacity (<5 kb), a single cell can be simultaneously transduced with multiple AAV vectors. In the present study, dual immunofluorescence staining showed efficient cotransduction of cells with different AAV vectors in the rat striatum, a finding consistent with that which we observed in a previous study [5].

Gene therapy strategies for the treatment of PD using AAV vectors include gene delivery of dopamine-synthesizing enzymes into the striatum to restore dopamine production, as well as gene delivery of neuroprotective molecules, such as glial cell line-derived neurotrophic factor, to block or slow down further degeneration [14]. In addition, AAV vectors harboring genes encoding neurotrophic factors might be delivered by intramuscular administration in an attempt to protect spinal motoneurons in patients suffering from amyotrophic lateral sclerosis [15–17]. Although no adverse effects due to overexpression of transgenes have been reported in animals to date, it is necessary to develop vectors that allow for regulation of transgene expression, thus avoiding transgene overexpression. In PD, overproduction of dopamine has the potential to cause dyskinesia or hallucinations, and sustained exposure to high concentrations of neurotrophic factors could result in tumor formation.

Inducible Cre recombinases have been used to generate a number of conditional knockout mice. They are invaluable tools for investigators studying the role of gene function in development, as well as a number of physiological and pathological processes. The tamoxifen-dependent $CreER^{T2}$ recombinase has proven particularly helpful [9,18,19]. It has been shown that 4-OHT does not alter dopamine content within the striatum in mice [20],

and we did not observe any adverse effects of 4-OHT treatment in the present experiment. In addition, tamoxifen, which is metabolized by the liver into 4-OHT, has neuroprotective effects [21,22]. Thus, the CreER^{T2} system might be useful for gene therapy in the treatment of neurological diseases.

We have expanded upon the use of inducible Cre recombinase technology to regulate transgene expression using an AAV vector-mediated gene delivery system. Recently, a viral vector-mediated RNA interference (RNAi) approach has been developed and localized gene knockdown achieved in the adult brain [23–25]. Although RNAi-mediated suppression of gene function has a wide variety of applications, more specific and inducible transgene silencing can be achieved with AAV-CreER^{T2}. Selective ablation of floxed transgenes reduces the possibility of down-regulation of normal cellular proteins. This system works as a molecular switch, increasing the safety of long-acting gene therapy by avoiding or minimizing side effects due to overproduction of the protein product and by providing the ability to shut down expression if toxicities are encountered or treatment is completed. The ability to restrict somatic recombination of transgenes spatially and temporally has a wide range of applications, in both gene therapy and biological study requiring somatic genetic manipulation.

Materials and Methods

AAV vector production. The AAV vector plasmids contained an expression cassette with a human cytomegalovirus immediate-early promoter (CMV promoter), followed by the first intron of human growth hormone, target cDNA, and a simian virus 40 polyadenylation signal sequence (SV40 poly(A)), between the inverted terminal repeats of the AAV-2 genome. The plasmids pAAV-LacZ, pEGFP, pAAV-AADC, pAAV-GCH, pCre, and pCreER^{T2} contained the cDNAs of LacZ, EGFP, human AADC, human GCH, Cre recombinase with a nuclear localization signal [26], and Cre recombinase fused to a mutated form of the ligand-binding domain of estrogen receptor α (CreER^{T2})[27], respectively. The plasmid pAAV-floxed TH contained human TH1 cDNA flanked by two loxP sequences between the CMV promoter and the SV40 poly(A). To generate pAAV-EGFP/Red, a DNA fragment containing d2EGFP (BD Biosciences, San Jose, CA, USA) and the SV40 poly(A) was flanked by loxP sequences and inserted between the CMV promoter and DsRed-Express-DR (BD Biosciences). The two helper plasmids, pHLP19 and pladeno1 (Avigen, Alameda, CA, USA), harbored the AAV *rep* and *cap* genes, as well as the *E2A, E4,* and *VA RNA* genes of the adenovirus genome, respectively. HEK293 cells were cotransfected by the calcium phosphate coprecipitation method with the vector plasmid, pHLP19, and pladeno1. The AAV vectors were then harvested and purified by two rounds of continuous iodoxale ultracentrifugations. Vector titers were determined by quantitative DNA dot-blot hybridization or by quantitative PCR of DNase I-treated vector stocks. We routinely obtained 10^{12} to 10^{13} vector genome copies (vg).

In vitro transduction. HEK293 cells were seeded at 3×10^5 cells/well in six-well plates. After 24 h, cells were infected with appropriate combinations of AAV vectors (5×10^9 vg per vector). 4-OHT was added to the culture medium at a concentration of 10 or 100 nM at 5 h after infection. Culture medium was collected for dopamine assay 48 h after infection and the cells were fixed for immunostaining.

AAV injections. All animal experiments were performed in accordance with the institutional guidelines. Three B6,129-*Gt(ROSA))26Sor*^{tm2Sho}/J mice (The Jackson Laboratory, Bar Harbor, ME, USA) [10] were stereotaxically injected into the caudoputaminal unit or cerebral cortex with 1×10^9 vg (1 μl) of AAV-CreER^{T2}. After 1 week, 4-OHT (1 mg) was administered intraperitoneally every day for 5 days, after which 2 of the mice were killed. One mouse that did not receive 4-OHT treatment was killed as a control. Creation of PD model rats and stereotaxic injections of AAV vectors were carried out as previously described [5]. Briefly, 60 male albino Wistar rats (weighing 200–250 g) were unilaterally lesioned at the left medial forebrain bundle (coordinates AP −4.3 mm and ML 1.6 mm, relative to the bregma, and DV −7.8 mm relative to the dura, with the incisor bar set 3.3 mm below the interaural line) with 4 μl of 4.5 mg/ml 6-OHDA HBr (Sigma, St. Louis, MO, USA) in 0.02% ascorbate saline prior to intrastriatal transduction. These rats were stereotaxically injected with AAV vectors (5×10^7 vg per site for each vector) at three sites in the lesioned striatum (coordinates relative to the bregma and dura, AP +1.5, +1.0, and +0.5 mm; ML 2.6, 3.0, and 3.2 mm; DV −5.2 mm). Forty-eight rats were injected with a 1:1:1 mixture of AAV-floxed TH, AAV-AADC, and AAV-GCH plus AAV-Cre (n = 12) or AAV-CreER^{T2} (n = 36). Twelve rats received AAV-LacZ alone as a control. Among the AAV-CreER^{T2}-treated rats, 24 were intraperitoneally injected with 4-OHT (4 mg/kg) for 5 consecutive days, starting either at the same time as or 4 weeks after vector injection.

Behavioral testing. The rats were tested weekly for rotational behavior and spontaneous limb use, as described previously [28]. The total number of complete body turns was counted during an observation period of ≥60 min following intraperitoneal injection of apomorphine HCl (0.1 mg/kg; Sigma). Only those animals exhibiting seven or more contralateral rotations/min in a 60-min period at 4 weeks after the 6-OHDA injection were included in further analysis. Spontaneous limb use was scored according to the cylinder test method [29]. Rats were placed in a clear glass cylinder large enough to ensure free movement. After they had performed 10 rears during which they were observed to place at least one paw on the cylinder wall, the number of times both forepaws contacted the wall of the cylinder was counted until at least 20 contacts were made. Data indicating the number of times a contralateral forepaw made contact with the wall are expressed as a percentage of the total. We also evaluated rotational behavior in response to a low dose of L-dopa methyl ester (5 mg/kg; Sigma) coadministered with 2.5 mg/kg of a peripheral decarboxylase inhibitor (benserazide hydrochloride; Sigma) 10 weeks after AAV injection.

Biochemical assays. Levels of dopamine in the cell culture medium (n = 4 for each group) and within the brain samples (n = 4 for each group) were determined by high-performance liquid chromatography (HPLC), as previously described [5]. Rats were killed by decapitation under sodium pentobarbital anesthesia 12 weeks after vector injection, after which their brains were immediately dissected and placed on dry ice. The striatum was punched out bilaterally using a sharp-edged, stainless steel tube. Wet tissue samples were weighed and stored at −80°C until subsequent analysis. Tissues were homogenized in 20 volumes of homogenization buffer and then mixed immediately with 0.76 M perchloric acid prior to centrifugation at 15,000*g* for 10 min. After the supernatant was neutralized with sodium acetate, the samples were analyzed by HPLC analysis. Determination of TH activity was based on the formation of L-dopa from L-tyrosine, as demonstrated by HPLC electrochemical detection. The reaction mixture contained 200 mM sodium acetate buffer (pH 6.0), 100 mM 2-mercaptoethanol, 0.2 mg/ml catalase, 0.2 mM L-tyrosine, and 1 mM tetrahydrobiopterin. The mixture was incubated for 10 min at 37°C. The reaction was stopped by adding perchloric acid, and L-dopa was extracted using an alumina column [30].

Immunostaining of cultured cells and brain sections. Cultured cells were fixed in 4% paraformaldehyde (PFA) in PBS. Brains were perfused with 4% PFA, soaked in 30% sucrose, and dissected into coronal sections (30 μm). The following primary antibodies were used: TH monoclonal (1:800 or 1:8000; DiaSorin, Stillwater, MN, USA) or polyclonal (1:10,000; provided by Ikuko Nagatsu, Fujita Health University, Japan), AADC polyclonal (1:10,000; I. Nagatsu), Cre recombinase monoclonal (1:500; Covance, Princeton, NJ, USA) or polyclonal (1:500; Covance), GFP polyclonal (1:200; BD Biosciences or Chemicon, Temecula, CA, USA), DsRed

doi:10.1016/j.ymthe.2005.08.009

polyclonal (1:1000; BD Biosciences), and GFAP (1:1000; Chemicon). Appropriate fluorescence-tagged (Invitrogen, Carlsbad, CA, USA) or biotinylated (Vector Laboratories, Burlingame, CA, USA) secondary antibodies were used for visualization. Immunoreactivity was assessed under microscopy (Axioplan, Zeiss, Germany) or confocal laser scanning microscopy (TCS NT; Leica Microsystems, Germany). To analyze quantitatively the numbers of TH-positive neurons and AADC-positive neurons, every 10th 30-μm section (total of 11 sections) covering a 3-mm thickness from each animal (n = 3 per group) was examined. Coexpression efficacy was analyzed by dual immunofluorescence staining.

Statistical analysis. One-way analysis of variance (ANOVA) was performed to determine differences in dopamine levels, as well as TH activity, followed by Tukey's test (StatView 5.0 software; Abacus). Behavioral changes were analyzed by a repeated measure ANOVA, followed by Tukey's test, with $P < 0.05$ considered statistically significant. Results are presented as means ± SEM.

ACKNOWLEDGMENTS

We thank Avigen, Inc., for providing the AAV vector production system. This work was supported by grants from the Ministry of Education, Science, Sports, and Culture, as well as by funds made available by the Japanese Government for a High-Tech Research Center Project for Private Universities (2003–2005) and a University–Industry Joint Research Project (2003–2005). In addition, we received grants from the Japan Ministry of Health, Labor, and Welfare; a grant from The Ministere de l'Education Nationale, de l'Enseignement Superieur et de la Recherche; and funds from The Cell Science Research Foundation, the Centre National de la Recherche Scientifique, the Institut National de la Santé et de la Recherche Médicale, and the Collège de France.

RECEIVED FOR PUBLICATION MAY 14, 2005; REVISED JULY 26, 2005; ACCEPTED AUGUST 1, 2005.

REFERENCES

1. Burton, E. A., Glorioso, J. C., and Fink, D. J. (2003). Gene therapy progress and prospects: Parkinson's disease. *Gene Ther.* **10:** 1721–1727.
2. Muramatsu, S., *et al.* (2003). Adeno-associated viral vectors for Parkinson's disease. *Int. Rev. Neurobiol.* **55:** 205–222.
3. Mandel, R. J., *et al.* (1998). Characterization of intrastriatal recombinant adeno-associated virus-mediated gene transfer of human tyrosine hydroxylase and human GTP-cyclohydrolase I in a rat model of Parkinson's disease. *J. Neurosci.* **18:** 4271–4284.
4. Muramatsu, S., *et al.* (2002). Behavioral recovery in a primate model of Parkinson's disease by triple transduction of striatal cells with adeno-associated viral vectors expressing dopamine-synthesizing enzymes. *Hum. Gene Ther.* **13:** 345–354.
5. Shen, Y., *et al.* (2000). Triple transduction with adeno-associated virus vectors expressing tyrosine hydroxylase, aromatic-L-amino-acid decarboxylase, and GTP cyclohydrolase I for gene therapy of Parkinson's disease. *Hum. Gene Ther.* **11:** 1509–1519.
6. Rajewsky, K., *et al.* (1996). Conditional gene targeting. *J. Clin. Invest.* **98:** 600–603.
7. Branda, C. S., and Dymecki, S. M. (2004). Talking about a revolution: the impact of site-specific recombinases on genetic analyses in mice. *Dev. Cell* **6:** 7–28.
8. Metzger, D., and Feil, R. (1999). Engineering the mouse genome by site-specific recombination. *Curr. Opin. Biotechnol.* **10:** 470–476.
9. Metzger, D., *et al.* (2003). Targeted conditional somatic mutagenesis in the mouse: temporally-controlled knock out of retinoid receptors in epidermal keratinocytes. *Methods Enzymol.* **364:** 379–408.
10. Mao, X., *et al.* (2001). Activation of EGFP expression by Cre-mediated excision in a new ROSA26 reporter mouse strain. *Blood* **97:** 324–326.
11. Sanchez-Pernaute, R., Harvey-White, J., Cunningham, J., and Bankiewicz, K. S. (2001). Functional effect of adeno-associated virus mediated gene transfer of aromatic L-amino acid decarboxylase into the striatum of 6-OHDA-lesioned rats. *Mol. Ther.* **4:** 324–330.
12. Tenenbaum, L., *et al.* (2004). Recombinant AAV-mediated gene delivery to the central nervous system. *J. Gene Med.* **6**(Suppl. 1)**:** S212–S222.
13. McCarty, D. M., Young, S. M., Jr., and Samulski, R. J. (2004). Integration of adeno-associated virus (AAV) and recombinant AAV vectors. *Annu. Rev. Genet.* **38:** 819–845.
14. Hurelbrink, C. B., and Barker, R. A. (2004). The potential of GDNF as a treatment for Parkinson's disease. *Exp. Neurol.* **185:** 1–6.
15. Azzouz, M., *et al.* (2004). VEGF delivery with retrogradely transported lentivector prolongs survival in a mouse ALS model. *Nature* **429:** 413–417.
16. Kaspar, B. K., *et al.* (2003). Retrograde viral delivery of IGF-1 prolongs survival in a mouse ALS model. *Science* **301:** 839–842.
17. Wang, L. J., *et al.* (2002). Neuroprotective effects of glial cell line-derived neurotrophic factor mediated by an adeno-associated virus vector in a transgenic animal model of amyotrophic lateral sclerosis. *J. Neurosci.* **22:** 6920–6928.
18. Imai, T., *et al.* (2004). Peroxisome proliferator-activated receptor gamma is required in mature white and brown adipocytes for their survival in the mouse. *Proc. Natl. Acad. Sci. USA* **101:** 4543–4547.
19. Simon, D., *et al.* (2004). Friedreich ataxia mouse models with progressive cerebellar and sensory ataxia reveal autophagic neurodegeneration in dorsal root ganglia. *J. Neurosci.* **24:** 1987–1995.
20. Kuo, Y. M., *et al.* (2003). 4-Hydroxytamoxifen attenuates methamphetamine-induced nigrostriatal dopaminergic toxicity in intact and gonadectomized mice. *J. Neurochem.* **87:** 1436–1443.
21. Ciriza, I., *et al.* (2004). Selective estrogen receptor modulators protect hippocampal neurons from kainic acid excitotoxicity: differences with the effect of estradiol. *J. Neurobiol.* **61:** 209–221.
22. Obata, T., and Kubota, S. (2001). Protective effect of tamoxifen on 1-methyl-4-phenylpyridine-induced hydroxyl radical generation in the rat striatum. *Neurosci. Lett.* **308:** 87–90.
23. Harper, S. Q., *et al.* (2005). RNA interference improves motor and neuropathological abnormalities in a Huntington's disease mouse model. *Proc. Natl. Acad. Sci. USA* **102:** 5820–5825.
24. Hommel, J. D., *et al.* (2003). Local gene knockdown in the brain using viral-mediated RNA interference. *Nat. Med.* **9:** 1539–1544.
25. Xia, H., *et al.* (2004). RNAi suppresses polyglutamine-induced neurodegeneration in a model of spinocerebellar ataxia. *Nat. Med.* **10:** 816–820.
26. Kalderon, D., Roberts, B. L., Richardson, W. D., and Smith, A. E. (1984). A short amino acid sequence able to specify nuclear location. *Cell* **39:** 499–509.
27. Feil, R., Wagner, J., Metzger, D., and Chambon, P. (1997). Regulation of Cre recombinase activity by mutated estrogen receptor ligand-binding domains. *Biochem. Biophys. Res. Commun.* **237:** 752–757.
28. Wang, L., *et al.* (2002). Delayed delivery of AAV-GDNF prevents nigral neurodegeneration and promotes functional recovery in a rat model of Parkinson's disease. *Gene Ther.* **9:** 381–389.
29. Schallert, T., *et al.* (2000). CNS plasticity and assessment of forelimb sensorimotor outcome in unilateral rat models of stroke, cortical ablation, parkinsonism and spinal cord injury. *Neuropharmacology* **39:** 777–787.
30. Nagatsu, T., Oka, K., and Kato, T. (1979). Highly sensitive assay for tyrosine hydroxylase activity by high-performance liquid chromatography. *J. Chromatogr.* **163:** 247–252.

Available online at www.sciencedirect.com
SCIENCE DIRECT®
Biochemical and Biophysical Research Communications 338 (2005) 1256–1262
BBRC
www.elsevier.com/locate/ybbrc

Transforming activity of the lymphotoxin-β receptor revealed by expression screening

Shin-ichiro Fujiwara [a,b,c], Yoshihiro Yamashita [a], Young Lim Choi [a], Tomoaki Wada [a], Ruri Kaneda [a,d], Shuji Takada [a], Yukio Maruyama [c], Keiya Ozawa [b], Hiroyuki Mano [a,d,*]

[a] *Division of Functional Genomics, Jichi Medical School, Tochigi 329-0498, Japan*
[b] *Division of Hematology, Jichi Medical School, Tochigi 329-0498, Japan*
[c] *First Department of Internal Medicine, Fukushima Medical University, Fukushima 960-1295, Japan*
[d] *CREST, Japan Science and Technology Agency, Saitama 332-0012, Japan*

Received 13 October 2005
Available online 24 October 2005

Abstract

Pancreatic ductal carcinoma (PDC) remains one of the most intractable human malignancies. To obtain insight into the molecular pathogenesis of PDC, we constructed a retroviral cDNA expression library with total RNA isolated from the PDC cell line MiaPaCa-2. Screening of this library with the use of a focus formation assay with NIH 3T3 mouse fibroblasts resulted in the identification of 13 independent genes with transforming activity. One of the cDNAs thus identified encodes an NH_2-terminally truncated form of the lymphotoxin-β receptor (LTBR). The transforming activity of this short-type LTBR in 3T3 cells was confirmed by both an in vitro assay of cell growth in soft agar and an in vivo assay of tumorigenicity in nude mice. The full-length (wild-type) LTBR protein was also found to manifest similar transforming activity. These observations suggest that LTBR, which belongs to the tumor necrosis factor receptor superfamily of proteins, may contribute to human carcinogenesis.

Keywords: Lymphotoxin-β receptor; Pancreatic ductal carcinoma; Retrovirus; cDNA expression library; Oncogene

Pancreatic ductal carcinoma (PDC) originates from pancreatic ductal cells and remains one of the most intractable human malignancies [1,2]. Effective therapy for PDC is hampered by the absence of specific clinical symptoms. At the time of diagnosis, most affected individuals are no longer candidates for surgical resection, and, even in patients who do undergo such surgery, the 5-year survival rate is only 20–30% [2].

The molecular pathogenesis of PDC has been the subject of intensive investigation. The gene *KRAS2* is frequently mutated and activated in PDC cells [3], and various tumor suppressor genes, including those for p53, p16, and BRCA2, are inactivated [4]. Furthermore, genetic or epigenetic alterations of genes important in apoptosis or in tumor cell invasion or metastasis have been detected in PDC cells [5]. However, mutations in *KRAS2* have also been identified in pancreatic tissue affected by nonmalignant chronic pancreatitis [6], and genetic changes truly specific to PDC remain to be uncovered. Improvement in the prognosis of individuals with PDC will require identification of the genetic or epigenetic alterations responsible for the aggressive nature of this cancer.

The focus formation assay with 3T3 or RAT1 fibroblasts has been extensively used to screen for transforming genes in various carcinomas [7]. Given that the expression of exogenous genes in this assay is usually controlled by their own promoters or enhancers, however, oncogenes are able to exert their transforming effects in the recipient cells only if these regulatory regions are active in fibroblasts, which is not always the case. Regulation of the transcription of test cDNAs by a promoter known to function efficiently in fibroblasts would be expected to

* Corresponding author. Fax: +81 285 44 7322.
E-mail address: hmano@jichi.ac.jp (H. Mano).

0006-291X/$ - see front matter © 2005 Elsevier Inc. All rights reserved.
doi:10.1016/j.bbrc.2005.10.080

ensure sufficient expression of the encoded protein in the focus formation assay. We have therefore now constructed a retroviral cDNA expression library from a human PDC cell line, MiaPaCa-2, and tested this library in the focus formation assay with 3T3 cells. For library construction, we took advantage of a polymerase chain reaction (PCR) system that preferentially amplifies full-length cDNAs. The resulting library had sufficient complexity with a high percentage of full-length cDNAs. With this library, we have revealed that the lymphotoxin-β receptor (LTBR) gene possesses transforming activity.

Materials and methods

Cell lines and culture. MiaPaCa-2, NIH 3T3, and BOSC23 cell lines were obtained from American Type Culture Collection and maintained in Dulbecco's modified Eagle's medium (DMEM)–F12 (Invitrogen, Carlsbad, CA) supplemented with 10% fetal bovine serum (Invitrogen) and 2 mM L-glutamine.

Construction of retroviral cDNA expression library. Total RNA extracted from MiaPaCa-2 cells with the use of an RNeasy Mini column and RNase-free DNase (Qiagen, Valencia, CA) was subjected to first-strand cDNA synthesis with PowerScript reverse transcriptase, SMART IIA oligonucleotide, and CDS primer IIA (Clontech, Palo Alto, CA). The resulting cDNAs were amplified for 14 cycles with 5′ PCR primer IIA and a SMART PCR cDNA synthesis kit (Clontech), with the exception that LA *Taq* polymerase (Takara Bio, Shiga, Japan) was substituted for the Advantage 2 DNA polymerase provided with the kit. The amplified cDNAs were treated with proteinase K, rendered blunt-ended with T4 DNA polymerase, and ligated to the BstXI-adaptor (Invitrogen). Unbound adaptors were removed with the use of a cDNA size-fractionation column (Invitrogen), and the remaining cDNAs were ligated into the BstXI site of the pMXS retroviral plasmid (kindly provided by T. Kitamura, Institute of Medical Science, University of Tokyo). The resulting pMXS-cDNA plasmids were introduced into ElecroMax DH10B cells (Invitrogen) by electroporation.

Focus formation assay. BOSC23 cells (1.8×10^6) were seeded into a 6-cm culture dish, cultured for 24 h, and then transfected with 2 μg of retroviral plasmids mixed with 0.5 μg of pGP plasmid (Takara Bio), 0.5 μg of pE-eco plasmid (Takara Bio), and 18 μl of Lipofectamine reagent (Invitrogen). Two days after transfection, polybrene (Sigma, St. Louis, MO) was added to the culture supernatant at a concentration of 4 μg/ml, and the supernatant was subsequently used to infect 3T3 cells for 48 h. The culture medium of the 3T3 cells was then changed to DMEM-F12 supplemented with 5% calf serum and 2 mM L-glutamine, and the cells were cultured for 2 weeks.

Recovery of cDNAs from transformants. Transformed 3T3 cell clones were harvested with a cloning syringe and cultured independently in 10-cm culture dishes. Genomic DNA was extracted from each clone by standard procedures and then subjected to PCR with 5′ PCR primer IIA and LA *Taq* polymerase for 50 cycles of 98 °C for 20 s and 68 °C for 6 min. Amplified DNA fragments were purified by gel electrophoresis and ligated into the pT7Blue-2 vector (EMD Biosciences, San Diego, CA) for nucleotide sequencing.

Anchorage-independent growth in soft agar. 3T3 cells (2×10^6) were infected with a retrovirus encoding a truncated form of LTBR or activated KRAS2 (see Results), resuspended in the culture medium supplemented with 0.4% agar [SeaPlaque GTG agarose (Cambrex, East Rutherford, NJ)], and seeded onto a base layer of complete medium supplemented with 0.5% agar. Cell growth was assessed after culture for 2 weeks.

Tumorigenicity assay in nude mice. 3T3 cells (2×10^6) infected with a retrovirus either encoding the truncated form of LTBR or containing the human wild-type LTBR cDNA (GeneCopoeia, Germantown, MD) were resuspended in 500 μl of phosphate-buffered saline and injected into each shoulder of a nu/nu Balb-c mouse (6-weeks old). Tumor formation was assessed after 3 weeks.

5′-Rapid amplification of cDNA ends (RACE). 5′-RACE was performed as described [8]. In brief, total RNA extracted from MiaPaCa-2 cells was used to generate cDNAs with an LTBR-specific primer (5′-GCAGTGGCTGTACCAAGTCA-3′). Excess primer was removed with a microconcentrator (Amicon, Austin, TX), and a poly(A) tail was added to the cDNAs by incubation with dATP and terminal deoxynucleotidyltransferase (Invitrogen). The first PCR was performed with the dT-adaptor primer (5′-GACTCGAGTCGACATCGATTTTTTTTTTTTT TTTT-3′) and RACE-1 antisense primer (5′-CTCCCAGCTTCCAGCT ACAG-3′), and the second PCR with the adaptor primer (5′-GACTCGA GTCGACATCG-3) and RACE-2 antisense primer (5′-GAGCAGAAA GAAGGCCAGTG-3′). The amplification protocol for the first PCR comprised incubation at 94 °C for 2 min followed by 20 cycles of 94 °C for 1 min, 55 °C for 1 min, and 72 °C for 3 min. That for the second PCR included incubation at 94 °C for 2 min followed by 30 cycles of 94 °C for 1 min, 53 °C for 1 min, and 72 °C for 3 min.The final PCR products were ligated into pT7Blue-2 for nucleotide sequencing.

Results

Screening for transforming genes by focus formation assay

To screen for transforming genes in PDC, we constructed a cDNA expression library from MiaPaCa-2 cells. Full-length cDNAs were selectively amplified by a PCR protocol from total RNA isolated from the cells and were ligated into the retroviral vector pMXS. We obtained a total of 1.2×10^6 colony-forming units of independent library clones, from which we randomly selected 30 clones and examined the incorporated cDNAs. An insert of $\geqslant 500$ bp was present in 24 (80%) of the 30 clones and the average size of these 24 inserts was 1.84 kbp.

Introduction of the library plasmids into a packaging cell line yielded a recombinant retroviral library that was used to infect mouse NIH 3T3 fibroblasts. After culture of the infected cells for 2 weeks, a total of 18 transformed foci were identified. No foci were observed for 3T3 cells infected with the empty virus. Each transformed focus was isolated, expanded, and used to prepare genomic DNA. PCR amplification of the inserts identified a total of 29 cDNA fragments, each of which was ligated into a cloning vector and subjected to nucleotide sequencing from both ends. Screening of the 29 cDNA sequences against the public nucleotide sequence databases revealed that they showed >95% sequence identity to 13 independent genes, 11 known and 2 unknown (Table 1).

To confirm the transforming ability of the isolated cDNAs, we again ligated them into pMXS and used the corresponding retroviral vectors to re-infect 3T3 cells. Two of the 13 independent genes (clone ID #4, corresponding to *LTBR* [GenBank Accession No. NM_002342]; clone ID #10, corresponding to *KRAS2* [GenBank Accession No. NM_004985]) reproducibly induced the formation of transformed foci in 3T3 cells (Fig. 1). Further sequencing our *KRAS2* cDNA revealed that it has a point mutation leading to the amino acid change from a glycine residue at position 12 to a cysteine (data not shown). Whereas the oncogenic potential of mutated *KRAS2* has been

Table 1
MiaPaCa-2 cell cDNAs isolated from 3T3 transformants

Clone ID #	Gene symbol	GenBank No.	Presence of entire ORF
1	CGI-152	NM_020410	Yes
2	RAB28	NM_004249	Yes
3	MRPL43	NM_032112	Yes
4	LTBR	NM_002342	No
5	UBQLN1	NM_013438	Yes
6	TBC1D2	NM_018421	Yes
7	FKBP10	NM_021939	Yes
8	HCCA2	NM_053005	Yes
9	Unknown	AK123415	ND
10	KRAS2	NM_004985	Yes
11	STK11IP	NM_052902	Yes
12	Unknown	AA627562	ND
13	PFKP	NM_002627	Yes

ORF, open reading frame; ND, not determined.

extensively investigated [3], little is known of such activity for *LTBR*. We thus focused on *LTBR* for further analysis.

Identification of a truncated form of LTBR

Although the nucleotide sequence of both ends of our LTBR cDNA was identical to that of human *LTBR*, the size of our cDNA (1452 bp) was smaller than that (2136 bp) of the full-length cDNA previously described. We thus determined the complete nucleotide sequence of our cDNA, revealing that it starts at nucleotide position 685 of the reported sequence (NM_002342). The longest open reading frame in our cDNA begins at amino acid position 221 and ends at position 435 of the previously described LTBR protein; it therefore encodes a predicted protein of 215 amino acids with a calculated molecular mass of 22,692 Da (Fig. 2). Given that the nucleotide sequence surrounding the putative translation start site of our cDNA matches the consensus Kozak motif, the corresponding mRNA likely produces this NH_2-terminally truncated form of LTBR, which is hereafter referred to as short-type LTBR.

5′-RACE analysis of LTBR mRNA

To confirm the presence of an mRNA encoding short-type LTBR in MiaPaCa-2 cells, we performed 5′-RACE to determine the 5′ ends of LTBR mRNAs. The first strand of LTBR cDNAs was generated with an LTBR-specific reverse transcription (RT) primer (Fig. 2) from RNA isolated from MiaPaCa-2 cells. Poly(A) was added to the 3′ end of the cDNAs, which were then subjected to nested PCR in order to amplify the 5′ ends. PCR products (ranging from a few hundred to 2000 bp) were detected only when reverse transcriptase was included in the procedure (Fig. 3A), indicating that the products were synthesized from cDNA, not from genomic DNA. The nucleotide sequence of 96 randomly chosen PCR products was determined. Sixty-eight of the 96 products matched the LTBR cDNA sequence and the positions of their 5′ ends are indicated in Fig. 3B. Transcription of most of the mRNAs corresponding to these PCR products was initiated in the region immediately upstream of the translation start site for short-type LTBR, indicating the existence of multiple mRNAs for this truncated protein in vivo.

Confirmation of transforming activity of short-type LTBR

To confirm the transforming activity of short-type LTBR, we examined its effect on anchorage-independent growth of 3T3 cells in soft agar. Whereas cells infected with an empty virus did not grow in soft agar, those infected with a virus encoding short-type LTBR formed multiple foci in repeated experiments (Fig. 4A). In addition, 3T3 cells expressing activated *KRAS2* readily grew in the agar.

We also injected the infected cells into nude mice. Tumors formed at all ($n = 10$) sites injected with 3T3 cells expressing short-type LTBR (Fig. 4B). Again, 3T3 cells expressing activated *KRAS2* also generated tumors at a high frequency, whereas those infected with the empty virus did not induce tumor formation. Together, these results thus confirmed that short-type LTBR possesses transforming activity.

Transforming activity of wild-type LTBR

To determine whether the full-length (435-amino acid) LTBR protein also possesses oncogenic potential, we performed the focus formation assay and in vivo tumorigenicity assay with a recombinant retrovirus encoding the wild-type

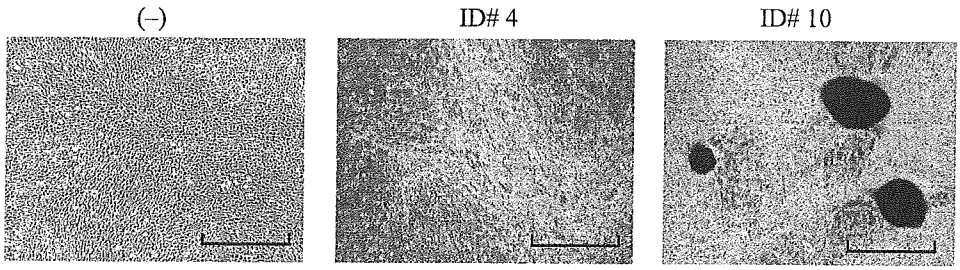

Fig. 1. Identification of transforming genes of MiaPaCa-2 cells. Mouse 3T3 cells were infected with an empty retrovirus (–) or with recombinant retroviruses harboring cDNAs corresponding to library clones ID #4 (short-type LTBR) or ID #10 (KRAS2). The cells were photographed after culture for 2 weeks. Scale bars, 1 mm.

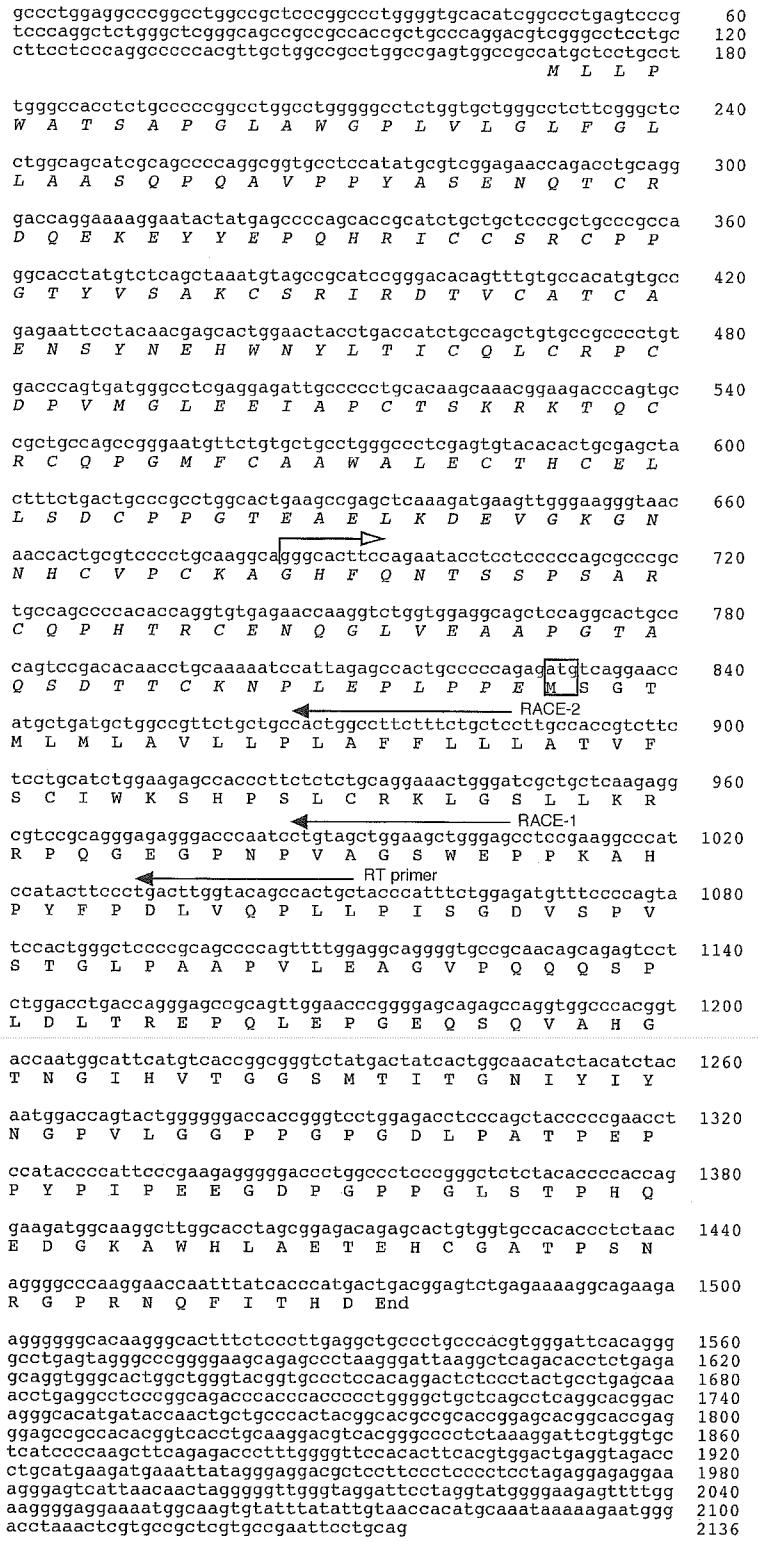

Fig. 2. Characterization of an LTBR cDNA isolated by screening for transformation activity. Amino acid residues of the full-length LTBR protein are aligned with the previously determined nucleotide sequence of LTBR cDNA (NM_002342). The cDNA isolated in the present study begins at nucleotide position 685 (open arrow) of the reported cDNA. The putative translation start site for the truncated (short-type) LTBR protein is boxed. The positions of primers used for 5′-RACE are indicated by closed arrows.

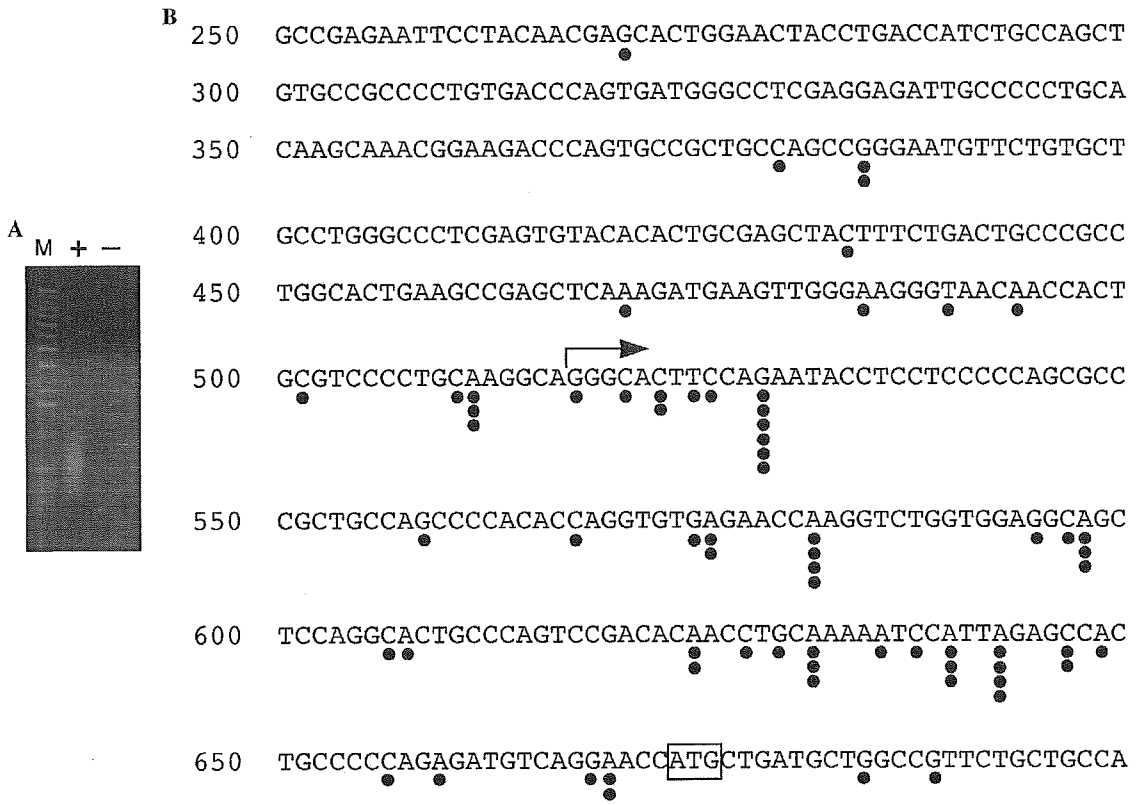

Fig. 3. 5′-RACE analysis of LTBR cDNA. (A) Total RNA of MiaPaCa-2 cells was incubated with the LTBR-specific RT primer in the presence (+) or absence (−) of reverse transcriptase, and resulting cDNA was subjected to PCR-based 5′-RACE. The PCR products were fractionated by electrophoresis through a 1.8% agarose gel and stained with ethidium bromide. Lane M, 1-kb DNA ladder. (**B**) The positions of the 5′ ends of 5′-RACE products are indicated by closed circles in alignment with the reported LTBR cDNA sequence. Numbers on the left indicate nucleotide positions relative to the translation initiation site of the full-length (wild-type) cDNA. The arrow indicates the 5′ end of the cDNA isolated by retroviral screening in the present study; the putative translation start codon of this cDNA is boxed.

human protein. The infected cells generated both transformed foci in vitro and tumors in nude mice (Fig. 5).

Discussion

In the present study, we constructed a retroviral cDNA expression library for a PDC cell line. Given that 80% (24/30) of the viral plasmids contained cDNA inserts and that the overall clone number was >1 million, this library should represent most of the mRNAs in MiaPaCa-2 cells. We infected 3T3 mouse fibroblasts with this recombinant library to screen for transforming genes with a focus formation assay. This screen identified *KRAS2* with an activating mutation as a transforming gene of MiaPaCa-2 cells, supporting the fidelity of our approach.

Our screen also identified a transforming cDNA that encodes an NH_2-terminally truncated form of LTBR. 5′-RACE analysis revealed the existence of mRNAs for this short-type LTBR in MiaPaCa-2 cells, and retrovirus-mediated expression of the isolated cDNA in 3T3 cells conferred the ability to grow in soft agar in vitro as well as the ability to form tumors in vivo.

LTBR belongs to the tumor necrosis factor (TNF) receptor superfamily [9] and binds two functional ligands, lymphotoxin-$\alpha 1\beta 2$ and LIGHT [10,11]. LTBR is expressed by many cell types (but not by lymphocytes), whereas expression of the LTBR ligands is restricted to activated lymphocytes [11]. Signaling by LTBR is important in the development of lymphoid tissue and in generation of adaptive humoral immune responses [12,13]. In general, LTBR function is thought to be linked to apoptosis. Indeed, activation of LTBR by its endogenous ligands or by anti-receptor antibodies triggers the death of various tumor cell lines [14,15]. Activation of the LIGHT-LTBR signaling pathway in tumor cells also induces marked chemokine-dependent recruitment of T cells to tumors, resulting in the rejection of established tumor cells [16].

LTBR activation has also been linked to tumor development, however. Its activation in fibrosarcoma cells thus induces angiogenesis and tumor growth by triggering the release of macrophage inflammatory protein-2, an angiogenic CXC chemokine [17]. Although oncogenic potential has not previously been demonstrated for LTBR, our data now show that both the full-length and truncated forms of this protein possess transforming activity even in the absence of exogenous cognate ligands. A high level of expression of LTBR conferred by the retroviral long terminal repeat in our experiments might have resulted in self-oligomerization